Ministry of Higher Education and Scientific Research
Ghardaïa University
Faculty of Science and Technology
Department of common teaching in science and technology

In order to obtain the degree of

MASTER

Domain: science of matter | Field: chemistry | Specialty: Analytical Chemistry

Theme:

Experimental study on the removal of Congo Red by adsorption using waste foundry sand

Publicly defended on 02/06/2025

Presented by :

- Ibtissem HABIB
- Romaissa DAHEUR

Jury Members:

Zohra BABAAMER	Pr	University of Ghardaia	President
Hadj Daoud BOURAS	MCA	University of Ghardaia	Supervisor
Yasmina KHANE	MCA	University of Ghardaia	Examiner
Mounir DAOUD	MCA	University of Ghardaia	Examiner

2024 / 2025

Abstract:

This work aimed to explore the potential of using waste foundry sand (WFS) as an adsorbent for the removal of Congo Red (CR) dye from aqueous solutions. As a low-cost, sustainable adsorbent. The adsorbent was characterized by X-Ray Diffractometer and Fourier Transformer Infrared Spectroscopy (FTIR) techniques, Boehm titration, and pH_{PZC}. The Box Behnken design (BBD) of experiments was applied to determine the influence of initial concentration (A), mass of adsorbent (B), and pH (C) for the CR dye elimination from the aqueous system. The significant interaction between the factors is BC with p-value < 0.05. The adsorption process followed pseudo-second-order kinetic model. The equilibrium data were fitted to Langmuir, Freundlich and Temkin isotherms. Based on R^2, the equilibrium adsorption data was better fitted to Langmuir isotherm model than any other model. The adsorption reached equilibrium after 60 min and the maximum adsorption capacity was about 36.16 mg/g at 20°C according to the Langmuir model. The results indicated that the removal efficiency of 20 mg/L CR reached approximately 90.49% and the adsorption yield is 62.34%. Thermodynamic parameters of the adsorption (ΔH°, ΔS° and ΔG°) were also determined and it was found that the adsorption of Congo Red by WFS was a spontaneous process and endothermic.

Keywords: Adsorption; Photocatalysis; Congo Red; Waste foundry sand.

Résumé:

Ce travail visait à explorer le potentiel d'utilisation de résidu de sable de fonderie (WFS) comme adsorbant pour l'élimination du colorant Rouge Congo (CR) des solutions aqueuses, en tant qu'adsorbant économique et durable. L'adsorbant a été caractérisé par les techniques de diffractométrie des rayons X (XRD) et de spectroscopie infrarouge à transformée de Fourier (FTIR), le titrage de Boehm et le pH_{PZC}. Le plan d'expériences Box Behnken (BBD) a été appliqué pour déterminer l'influence de la concentration initiale (A), de la masse d'adsorbant (B) et du pH (C) sur l'élimination du colorant CR du système aqueux. L'interaction significative entre les facteurs est BC avec une valeur de $p < 0,05$. Le processus d'adsorption a suivi une cinétique de pseudo-deuxième ordre. Les données à l'équilibre ont été ajustées aux isothermes de Langmuir, Freundlich et Temkin. Sur la base du R^2, les données d'adsorption à l'équilibre se sont mieux ajustées au modèle isotherme de Langmuir qu'à tout autre modèle. L'adsorption a atteint l'équilibre après 60 min et la capacité maximale d'adsorption était d'environ 36,16 mg/g à 20°C selon le modèle de Langmuir. Les résultats ont indiqué que l'efficacité d'élimination du CR à 20 mg/L atteignait environ 90,49% et que le rendement d'adsorption était de 62,34%. Les paramètres thermodynamiques de l'adsorption ($\Delta H°$, $\Delta S°$ et $\Delta G°$) ont également été déterminés et il a été constaté que l'adsorption du Rouge Congo par le WFS était un processus spontané et endothermique.

Mots clés: Adsorption; Photocatalyse; Rouge Congo; Résidu de sable de fonderie.

ملخص:

الهدف من هذه الدراسة هو التحقق من امتزاز صبغة الكونغو الحمراء (CR) من المحاليل المائية باستخدام رمال المصانع المستهلكة (WFS) كمادة ممتّزة منخفضة التكلفة ومستدامة. وُصفت المادة الممتّزة باستخدام مقياس حيود الأشعة السّينية، وطيف الأشعة تحت الحمراء (FTIR) ومعايرة Boehm وpH_{PZC}. طُبق تصميم Box Behnken (BBD) للتجارب لتحديد تأثير التركيز الابتدائي للملون (A)، والكتلة الحيوية للمادة الممتّزة (B)، ودرجة حموضة المحلول (C) على إزالة صبغة الكونغو الحمراء من المحاليل المائية. التأثير الهام بين العوامل هو BC بقيمة احتمالية < 0.05. اتبعت عمليات الامتزاز الحيوي حركية معدل شبه من الدرجة الثانية (PSO). تمت دراسة ايزوتارم التفاعل وفقًا لمعادلة لانغمير، وفرويندليش، وتمكين. بناءً على R^2، كانت بيانات الايزوتارم أكثر ملاءمةً لنموذج لونغمير من أي نموذج آخر. وصل الامتزاز إلى حالة التوازن بعد 60 دقيقة، وبلغت أقصى سعة الامتزاز حوالي 36.16 ملغم/غم عند 20 درجة مئوية وفقًا لنموذج لانغمير. أشارت النتائج إلى أن كفاءة الإزالة الحيوية لـ 20 ملغم/لتر من CR بلغت حوالي 90.49%، وأن عائد الامتزاز هو 62.34%. كما حُددت الدراسة الديناميكية الحرارية للامتزاز($\Delta H°$ و $\Delta S°$ و $\Delta G°$) ووُجد أن امتزاز أحمر الكونغو بواسطة WFS كان عملية تلقائية وماصة للحرارة.

الكلمات المفتاحية: الامتزاز؛ التحفيز الضوئي؛ أحمر الكونغو و رمال المصانع المستهلكة.

Acknowledgments

Praise be to God, by whose grace good deeds are accomplished, and by whose grace aspirations are realized.

We thank the Almighty and Merciful Lord who granted us patience, courage, and wisdom.

The will to carry out this work is essential.

We extend our sincere thanks and appreciation to everyone who contributed to the completion of this scientific work, especially:

Our supervisor, **Dr. Hadj Daoud BOURAS**, for his availability, rigor, valuable advice, assistance, and attention.

We would also like to thank the members of the discussion committee, including the examiner , **Dr.KHANE Yasmina**, **Dr.DAOUD Mounir** and the president **Pr. BABAAMER Zohra**, for their time.

We are deeply grateful to the laboratory members for their support and encouragement.

We would also like to thank the members of the discussion committee.

We would also like to thank all the teachers who taught us over the past years, who provided us with the necessary tools to succeed in our studies.

Finally, it is important to also thank all the people who contributed directly or indirectly to the completion of this work.

Dedication

To my beloved mother,

Your eternal love, support, and countless sacrifices are the foundation of my success.

To my dear father,

You made this road so much easier with your support and guidance.

To my little brother Mohamed Taher,

You bring joy and inspiration into my life every single day.

To both of my grandmothers,

Losing you this year has left an emptiness and pain in me that words cannot fill. Yet, your love and wisdom continue to live within me. Every achievement I celebrate carries the echo of your presence. I only wish you were here to share in this moment.

To all the Taouti and Habib families,

Thank you for your constant encouragement and presence.

To all my friends,

Thank you for the laughter, the encouragement, and your companionship through this years.

And finally,

To my dearest binomial, Romaissa, who walked this path with me.

Sharing this work with you has been both a privilege and a joy. Your friendship means more to me than words could ever convey

Ibtissem

Dedication

I dedicate my graduation to those who have waited for this moment to be proud of me, to those who taught me patience and success, and to my dear parents.

To my beloved mother, Khaira, the source of compassion, who has been and continues to be the first supporter in my life.

All thanks to my dear father, Madjid, my eternal support and source of strength. I thank him for his continuous efforts in providing the best conditions for me. I pray to God to protect them and prolong their lives.

I also extend my thanks to my sisters, Aya and Feriel, and to my brother Oussama, who have never stopped encouraging and supporting me throughout my studies. May God protect you and grant you success.

To my friend and partner in this work, Ibtissem, who has been an example of diligence and cooperation. I ask God to grant her success in her life and continued achievements.

I also thank my friends: Nessrine, Amani, Meriem, Zahra, and Kawthar**.**

Romaissa

List of Figures

List of Tables

List of abbreviations

WFS: Waste Foundry Sand

ANOVA: Analysis of variance

CR: Congo red

pH: Hydrogen potential.

pHpzc: Hydrogen potential at the point of zero charge.

UV: Ultra-violet.

FTIR: Fourier- transform infrared spectroscopy

XRD: X-ray diffraction

Content

General introduction

General introduction

Water is a fundamental resource vital to human survival. as well as the aquatic flora and fauna [1]. It regulates climate, nourishes plants, sustains animals, and is vital for countless biological and chemical processes while water blankets 75% of the Earth's surface, only a limited portion exists as clean water, fresh, and accessible for human and ecological needs [2]. due to increasing industrialization, urban growth, and human activities which leads to the contamination of water resources [1].

Among the most harmful pollutants are synthetic dyes discharged by industries such as textiles, paper, cosmetics, pharmaceuticals, food, and leather, with annual releases exceeding 50,000 tons of organic pigments into the environment each year [3] including toxic compounds like Congo Red, these dyes are highly visible even at very low concentrations [4].

In order to reduce this growing problem various physical, chemical, and biological techniques have been developed over time [5]. Among all these techniques, adsorption is considered as one of the popular and attractive technologies for the removal of dyes from water [6]. It is the most favourable method due to its simple design [7], low cost and easy desorption [8]. Photocatalysis is another method which uses UV light to break down dye molecules into harmless by-products.

Recently, research has focused on sustainable and low-cost adsorbents, such as fungi [4], agricultural wastes [8], and industrial wastes.

One of those materials used is waste foundry sand (WFS) a by-product of the metal casting industry. Utilizing WFS as an adsorbent transforms waste into a useful resource, supporting both pollution control and waste valorization [1].

The aim of this study is to develope a cost-effective adsorbent made from waste foundry sand to remove Congo Red dye from aqueous solutions using adsorption and then compare it with the photocatalysis process. The research is divided into three key chapters:

- ✓ The first one is a bibliographic study, which is divided into three main parts: the waste foundry sand, dyes and the treatment methods used.
- ✓ Then the second chapter is a small description of the methods and the materials used in this work.
- ✓ The last one is a detailed discussion of the results obtained, followed by a general conclusion which summarize all the key findings.

Chapter I

Bibliographic study

Part 1:

Waste foundry sand

I. Bibliographic study

I.1. Waste foundry sand

I.1.1. Introduction

The growing demand for metal products has made casting one of the most important manufacturing processes. In casting, molds and cores made from special sand are used to shape molten metal into precise designs, this sand called foundry sand.

Foundry sand is the primary material used to create sand molding boxes. These boxes are formed by pressing two molds, one on top and one on the bottom, filled with compacted sand, against a solid object made of wood, plastic, or metal. This object serves as a replica of the part to be made. After pressing, the molds are briefly separated to remove the part, and then reassembled to form a mold with a cavity inside. Molten metal is poured into the mold, where it cools and hardens. The sand box is then removed and mechanically broken apart for reuse. The sand is reused multiple times usually between 3-10 cycles until it loses its effectiveness [9].

As shown in Figure I-1, the metal casting process involves a series of steps that transform raw materials into finished metal products through melting, molding, and solidification.

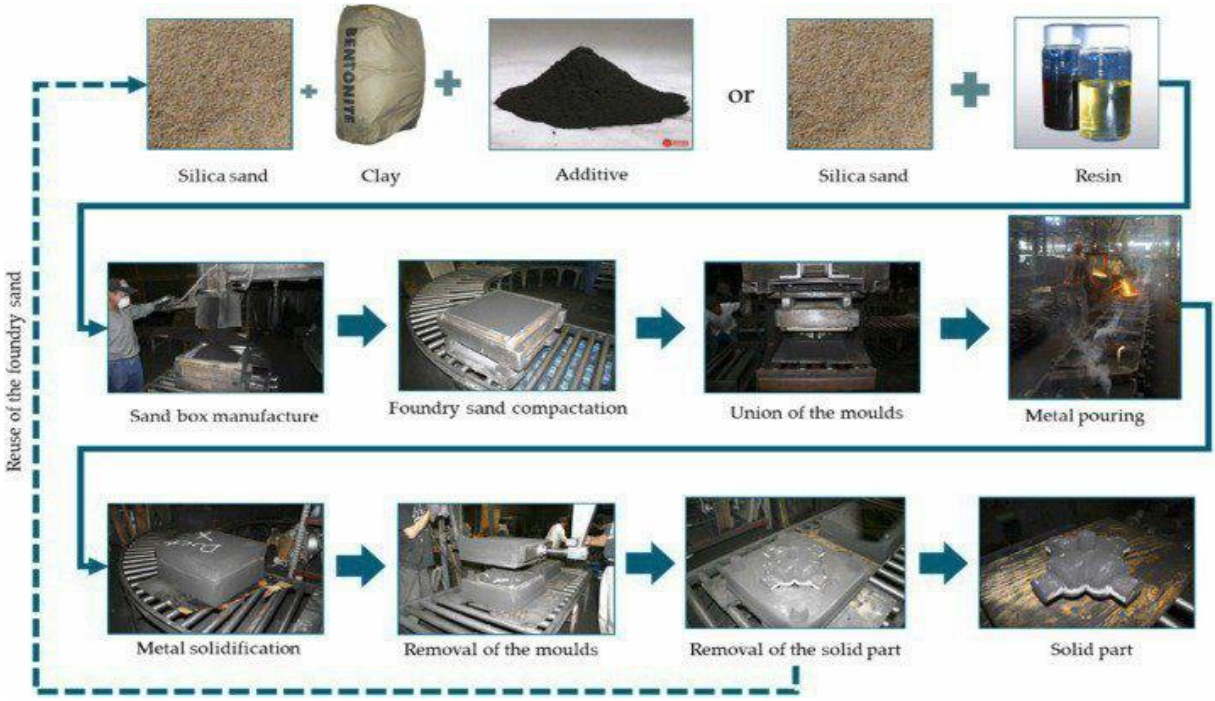

Figure I- 1: Metal casting process [9].

When the sand's properties degrade and it can no longer be used, it is termed waste foundry sand (WFS) and is often dumped in landfills. Approximately 100 million tons of WFS are produced annually, with 0.60 tons generated for every ton of steel made. The removal of WFS

has emerged as a major environmental concern due to limited landfill space and rising land costs.

I.1.2. Definition

Waste foundry sand (WFS) is a by-product of ferrous (iron and steel) and nonferrous (copper, aluminium, and brass) metal casting processes. It is primarily used in the formation of molds for casting metals. After the casting process, the sand becomes contaminated with residues from metals and binders, this makes it unsuitable for further use. WFS is composed mainly of silica, binders, metal traces, and catalysts.

I.1.3. Classification

Foundry sands are classified into two main types depending on the type of binders used to hold the sand grains together.

I.1.3.1. Green sand (wet sand)

Also called molding sand, uses clay as the binder. It is the most commonly used type of sand in foundries, typically used for smaller or medium sized castings. This type is preferred because of its flexibility and ease of recycling within the foundry.

Green sand is made up of silica (85-95%), bentonite clay (4-10%), carbonaceous additives (2-10%), and (2-5%) water. It is basically black in colour, due to carbon content. The term "green" refers to the fact that the sand mold is moist or "green" before the metal is poured into it. The high content of silica sand resists high heat, and clay helps hold the sand together [1].

I.1.3.2. Chemically bonded sand

Chemically bonded sands are used in core making, where they need to be strong enough to handle the heat from molten metal, and in mold making. Most chemical binder systems use an organic binder that is activated by a catalyst, although some systems use inorganic binders. These sands are usually lighter in colour and texture compared to the green sand.

The choice between green sand and chemically bonded sand depends on factors such as the type of metal being cast, the desired properties of the final product, and economic considerations (Green sand is generally lower cost compared to chemically bonded sand) [1].

Figure I-2 illustrates the two main types of waste foundry sand (WFS), namely (a) green sand and (b) chemically bonded sand.

(a) (b)

Figure I- 2: Types of WFS (a) green sand (b) chemically bonded sand.

I.1.4. Chemical and physical properties

The properties of WFS depend on variables such as the type of foundry process implemented, the type and amount of additives used for molding, the number of times the sand has been reused [9].

I.1.4.1. Chemical properties

- ✓ WFS can contain more than 80% of SiO_2, small percentage of Fe (9%) and Al (6%), these percentages can change depending on the product of the industry.
- ✓ Contain organic and inorganic compounds due to the type of binders.
- ✓ WFS has a hydrophilic nature and can absorb water.
- ✓ It can contain traces of MgO, K_2O, and TiO_2.
- ✓ We can found metal such as include Ag, Cd, Co, Cu, Fe and Ti due to the metal casting process [10].
- ✓ The pH of waste foundry sand can vary between 4 and 8 [11].

I.1.4.2. Physical proprieties

- ✓ The shape of WFS is generally subangular to round.
- ✓ The grain size distribution is from 85–95% for materials ranging between 0.6 mm and 0.15 mm, and 5–12% for those who are smaller than 75 µm.
- ✓ The density is between 220 and 2700 kg/m^3 [12].

I.1.5. Different applications of waste foundry sand

- ✓ We can use the WFS in the embankments and barrier layers construction because it develops compaction and reduces settlement.

- ✓ It can be used also in agriculture, soil reinforcement (it enhances soil aeration).
- ✓ WFS can be replaced the fine aggregates (typically river sand) in mortar mixes [11].
- ✓ Finally it can use in water treatment due to its adsorption property.
- ✓ We can use WFS in fiberglass manufacturing as a partial replacement for raw silica sand.

Part 2:

Dye

I.2. Dyes

I.2.1.Introduction

Throughout history, humans have been fascinated by colours, which have been an important part of art, decoration, craftsmanship, and dyeing.

In ancient times, people lean on natural pigments sourced from coloured earth, plants, and animals to add brightness to their atmosphere and enhance their daily lives. These natural dyes, like alizarin from madder plants and indigo sourced from wood or indigo plants, known as the foundation for early dyeing practices. Minerals such as manganese oxide and hematite also played a role in creating rich hues.

Everything changed in 1856 when William Henry Perkin created the first synthetic dye, "mauve" using aniline [13]. This innovation marked the beginning of a new era in dyeing, as synthetic dyes offered greater brightness, enhanced durability, and lower production costs compared to their natural counterparts. Today, most dyes are made from chemicals found in materials like petroleum and tar.

However, the elimination of these dyes into the environment, especially in water, has caused significant pollution. These dyes can harm aquatic life and even humans because many are toxic and some may even be cancer causing. As a result, there are strict regulations on their use, especially in products that come into contact with people.

I.2.2. Definition

A dye, whether natural or synthetic, is a substance that imparts long lasting colouration to materials. Dyes are composed of three parts [13]:

Chromophores: The active site responsible for absorbing light in the visible (380–750 nm), giving the dye its colour. Contains specific atomic groups that enable light absorption making the molecule chromogenic.

Auxochromes: Functional groups that enhance dye's properties by improving solubility, the ability to bond with materials and colour intensity.

Matrix: The rest of the molecule, providing structural support to the chromophore and auxochrome. Unlike dyes, which remain on the surface, pigments dissolve and disperse in their medium, changing their colour by binding to solid surfaces such as textiles through processes such as dyeing or printing. Their vibrant colours and strong fixing ability make them indispensable in various industries, from textiles to food and cosmetics [14].

Table I.1 lists the main chromophore and auxochrome groups commonly found in dye molecules.

Table I- 1: Main chromophores and auxochromes groups[14].

Chromophores Groups	Auxochromes Groups
Azo (-N=N-)	Primary Amine ($-NH_2$)
Carbonyl (>C=O)	Secondary Amine (-NHR)
Nitro ($-NO_2$)	Tertiary Amine ($-NR_2$)
Nitrous(-N=O)	Hydroxy (-OH)
Thiocarbonyl (>C=S)	Alkoxy (-OR)
Vinyl (-CH=CH-)	Electron Donor (-Cl)

I.2.3. Classification

To better understand their properties and applications, dyes are generally classified according to their origin, chemical structure, and method of application.

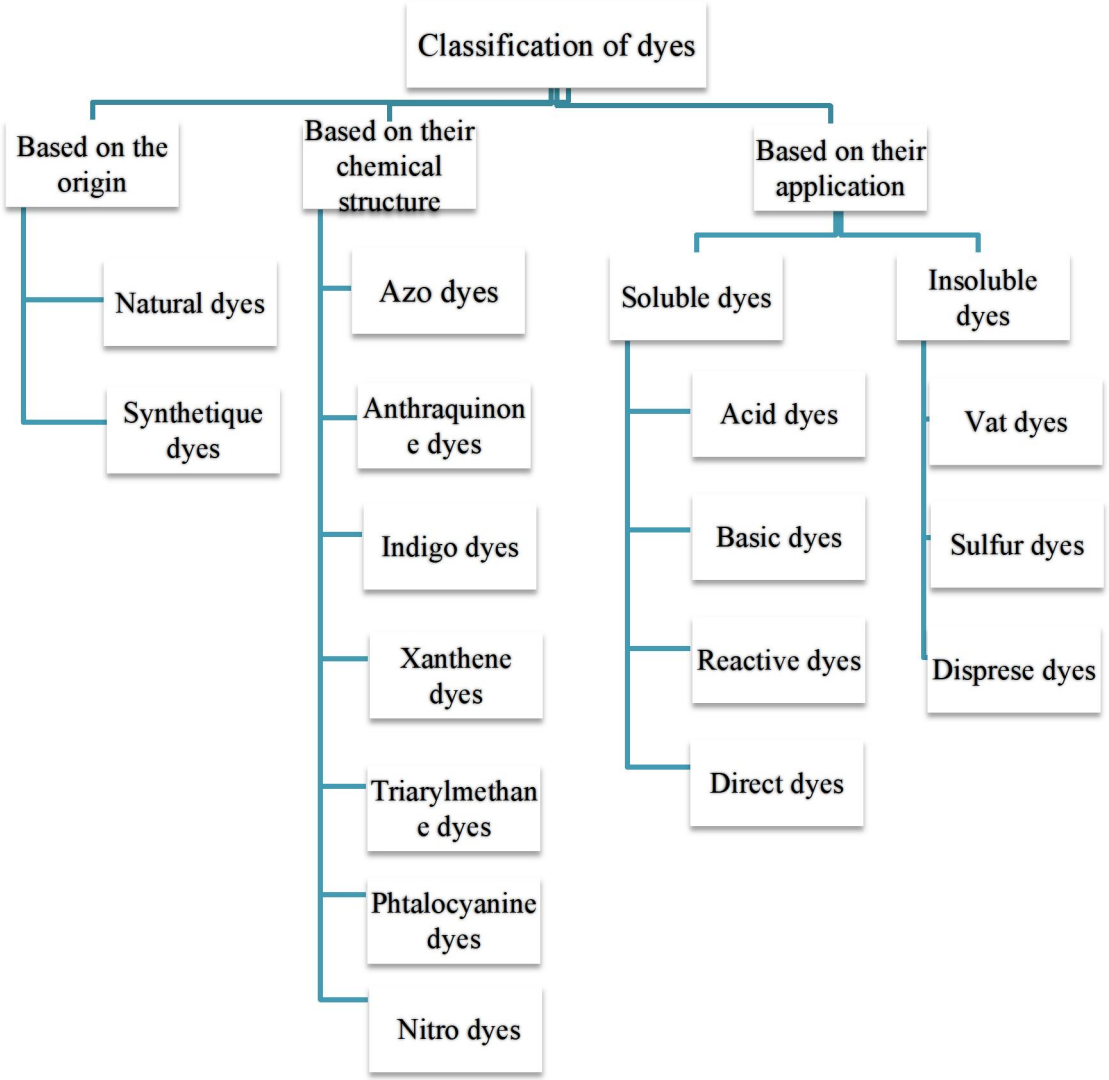

I.2.3.1. Based on the origin

Dyes may be classified into two categories, defined by the source from which they arise:

a. Natural dyes

They are obtained from the natural sources like animals, and mineral sources but most of them are sourced from the plants or plant parts like roots, leaves, bark, berries, wood, fungi, and lichens [5].

b. Synthetic dyes

They are produced on a wider scale using chemical synthesis and are widely manufactured by the dye industry. Its introduction has revolutionized the textile and fashion industries by providing a wider range of colour options, improved dyeing efficiency, and faster production processes**.**

Dyes may also be classified in different ways based on their chemical structure and types of applications [5].

I.2.4. Based on their chemical structure

This rests upon the chemical composition of the dyes, focusing especially on the essence of their chromophore groups [15].

a. Azo dyes

These dyes stand as the most prevalent in use, comprising nearly half of all commercial dyes, owing to their vivid hues, versatile structures, and straight forward synthesis. They are distinguished by the presence of azo groups (—N=N—) as illustrated in Figure I-3, bonded to electron-donating entities such as amine or hydroxyl groups, alongside electron-accepting aromatic rings an arrangement that underpins their brilliant colours and wide ranging applications [7].

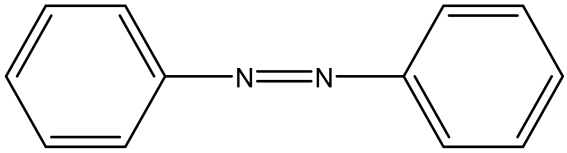

Figure I- 3: Structure of azo dye

b. Anthraquinone dyes

Ranked as the second largest class of dyes after azo dyes, anthraquinone dyes are extensively employed in the textile industry, celebrated for their distinctive chromophore groups. These groups are defined by two carbonyl moieties flanking a central benzene ring as shown in Figure I-4. Derivatives of anthraquinone dyes may contain amino, hydroxyl, halogen, or sulfonic acid groups [7].

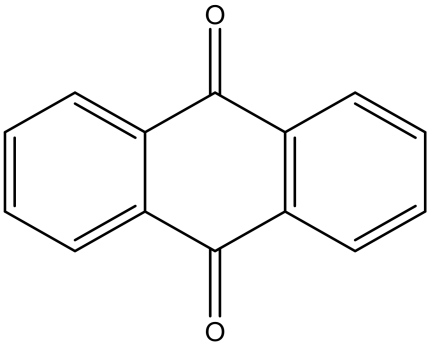

Figure I- 4: Structure of anthraquinone.

c. Indigo dyes

Indigo dyes trace their origins to the legendary deep blue pigment indigo, revered for centuries. Variants containing selenium, sulfur, or oxygen congeners of indigo blue induce notable chromatic transformations, often diminishing colour intensity or altering its hue, yielding shades that range from vibrant orange to serene turquoise [15].

The Figure I-5 presen the structure of indigo blue dye.

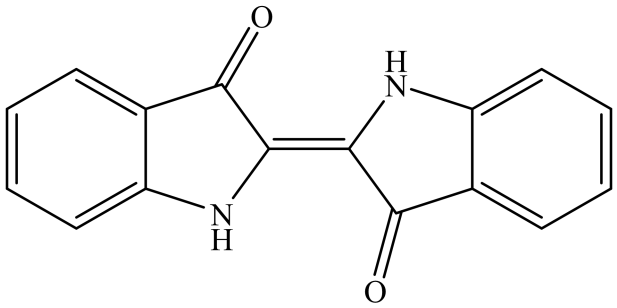

Figure I- 5: Structure of indigo blue.

d. Xanthene dyes

Xanthene dyes are known for their intense fluorescence, these dyes are used in different fields such as scientific field, industrial and environmental. The most known example is Fluorescein which is used as a tracer in maritime accident and underground water studies, Rhodamine B is another example used for tagging biological samples [5].

their molecular structure is shown in Figure I-6.

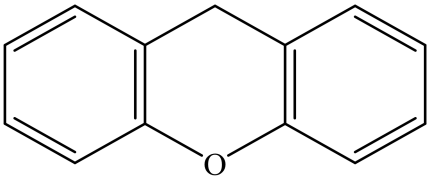

Figure I- 6: Structure of xanthene dye.

e. Triarylmethane dyes

This class of dyes is widely employed across the textile industry, cosmetics, and food colouring, owing to their remarkable light absorbing properties. They are defined by a central carbon atom bonded to three aryl groups as seen in Figure I-7. Among the most notable examples are Malachite Green, used in dyeing silk and leather, and Crystal Violet, commonly utilized in laboratories for staining cells and tissues [4].

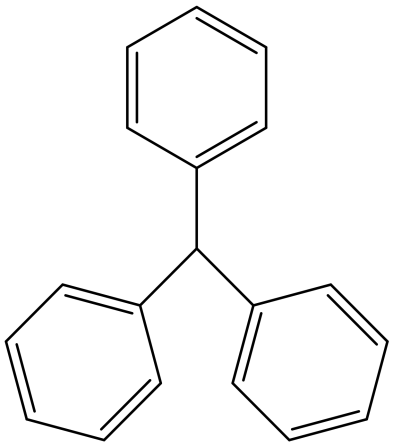

Figure I- 7: Structure of triarylmethane dye.

f. Phthalocyanine dyes

Phthalocyanine dyes are synthesized through the reaction of dicyanobenzene with metals such as copper, nickel, cobalt, or platinum. Among them, copper phthalocyanine stands out as the most widely used, prized for its exceptional chemical stability. Typically exhibiting vivid blue or green hues, these dyes find frequent application in textile coatings, plastics, and artistic materials, valued not only for their brilliance but also for their low toxicity [7]. Their structure is presented in Figure I-8.

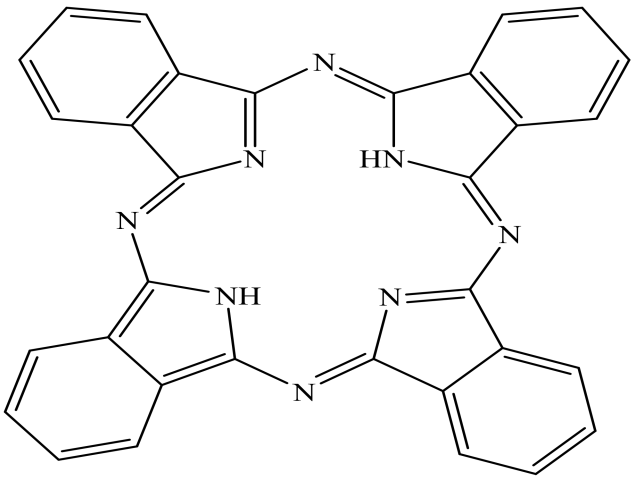

Figure I- 8: Structure of phthalocyanine dye.

g. Nitro dyes

Nitro dyes are characterized by the presence of nitro groups (NO_2) positioned ortho to electron-donating groups such as hydroxyl or amino moieties as seen in Figure I-9. Though their use in dyeing and printing persists, these dyes pose significant environmental risks, often polluting water bodies and endangering aquatic life. Despite being scarce and largely considered outdated, they endure in various applications due to their simple molecular structure and low production cost. Notable examples include Picric Acid, which serves both as a yellow dye and a potent explosive, and naphthol yellow S, formerly used in food production [5].

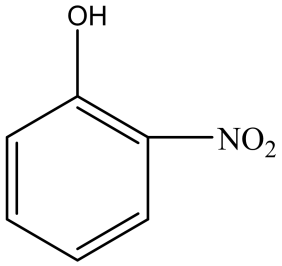

Figure I-9: Structure of nitro dye.

I.2.4.1. Based on application

Dyes are classified based on their auxochromes, which is useful for dyers who focus on practical applications. This classification considers dye solubility, affinity for different fibers, and fixation method [15].

Within this classification, dyes are grouped into two primary families: those that are water-soluble and those that are water-insoluble [15].

I.2.4.1.1. Soluble dyes

a- Acid or an anionic dye

Acid dyes or anionic dyes are the type of dyes used in acidic pH ranging between 2 to 6, these dyes are used for dyeing fibers like wool and cotton. These dyes are characterized by their sulfonic acid groups that made them water soluble and typically azo, anthraquinone and xanthenes types. Acidic dyes are widely used in textile industry, making up 30% to 40% of the total utilization of dyes due to their vibrant and good colour fastness [1].

The Figure I-10 present a structure of an acidic dye.

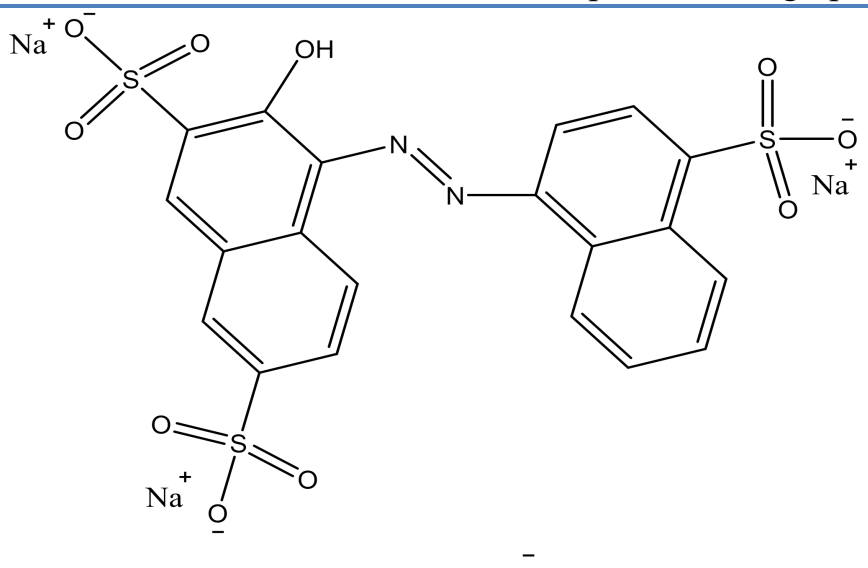

Figure I- 10: Structure of red acid dye.

b- Basic or Cationic dye

Perkin's Mauve was the first synthetic dye and belongs to the basic dye class. Other early examples of basic synthetic dyes include Magenta and Malachite Green. These dyes are derived from organic bases and ionize in water to form coloured cations, which is why they are classified as basic or cationic dyes, their general structure is shown in Figure I-11. Typically, cationic dyes are available in the form of salts, most commonly chlorides, but also as oxalates or double salts containing zinc chloride. Their remarkable intensity and brightness are among their most distinctive properties [6].

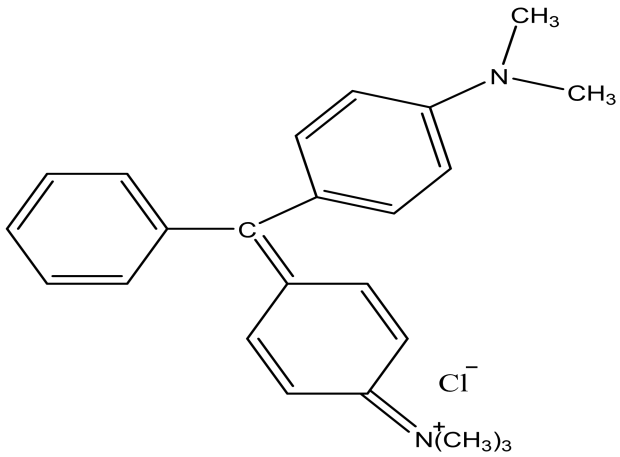

Figure I- 11: Structure of green 4 basic dye.

c- Reactive dyes

The chromophoric structures of reactive dyes are drawn from the azo, anthraquinone, and phthalocyanine families, lending them their vivid colouration and reactivity. They called reactive dyes because they have reactive chemical functions like triazine or vinylsulfone,

which form strong covalent bonds with fibres. These dyes are highly water-soluble and generally used for dyeing cotton, wool, and polyamides [15]. A typical structure is illustrated in Figure I-12.

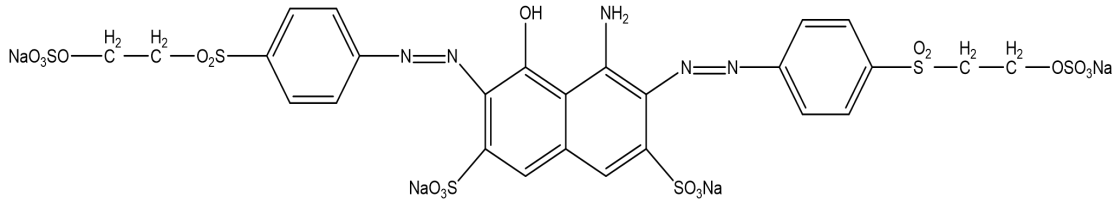

Figure I- 12: Structure of reactive black.

d- Direct dyes

Direct dyes are used for dyeing rayon, linen, and other cellulosic fibers, and they can also be applied to wool and silk. These dyes bind loosely to fiber molecules, preventing rapid drying after application. They are usually used at temperatures ranging from 79.4 °C to 93.3 °C [16]. Due to lack of fixative properties, fabrics dyed with direct dyes can only be cold washed. One of the key advantages of direct dyes is their cost-effectiveness, making them the most affordable option of all dye types [7]. Their strcture is presented in Figure I-13.

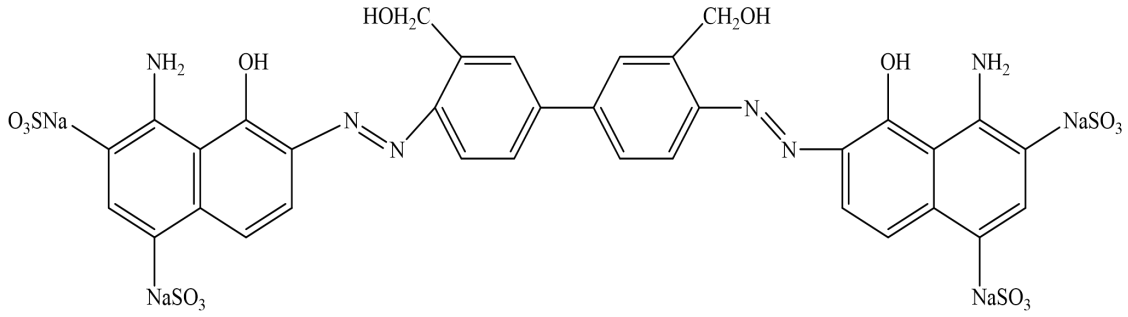

Figure I- 13: Structure of direct blue.

I.2.4.1.2. Insoluble dyes in water

a- Vat dyes

Vat dyes are renowned for their brilliant hues and exceptional colour fastness. Though inherently water-insoluble when affixed to fibers, they become soluble in an alkaline medium through a reduction process that transforms them into leuco-derivatives water-soluble forms. Once absorbed into the fibers, they are re-oxidized, returning to their original insoluble state.as seen in Figure I-14 Their remarkable resistance to washing and sunlight makes vat dyes ideal for colouring cotton, linen, wool, silk, rayon, and other cellulosic materials. Among them, indigo stands as the most iconic natural vat dye, widely used in the dyeing of denim [6].

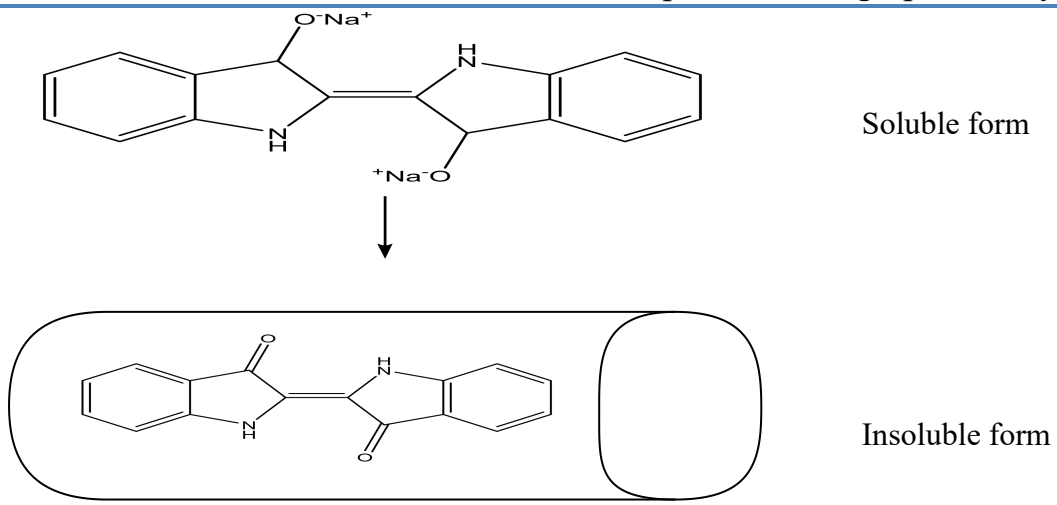

Figure I- 14: Structure of vat dye.

b- Sulfur dyes

Sulfur dyes are water-insoluble colorants distinguished by the presence of sulfur atoms in their structure and a notably high molecular weight. Though inherently insoluble, they are applied in a reduced, water-soluble form typically achieved through treatment with sodium sulfide. Once absorbed by the fiber, they are re-oxidized to restore their original insoluble state. Owing to their affordability and ability to produce deep, durable shades with strong resistance to washing and light, sulfur dyes are commonly used in cotton dyeing. First introduced in 1873, these dyes accounted for 9.1% of dye production in the United States by 1966 [6]. The structure of a sulfur dye is shown in Figure I-15.

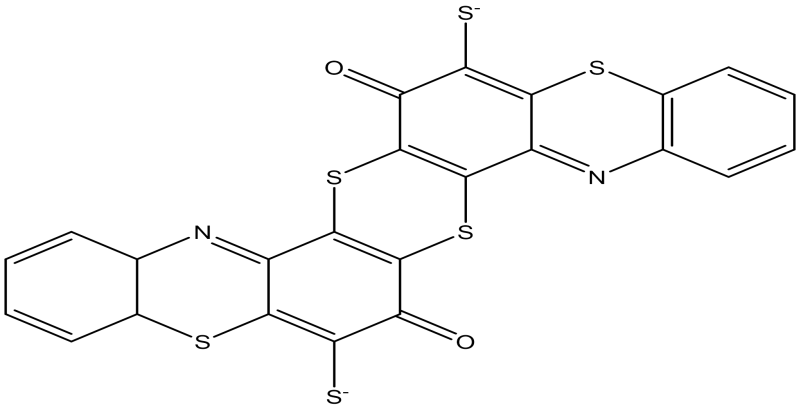

Figure I- 15: Structure of sulfur black 1.

c- Disperse dyes

Disperse dyes are water-insoluble, non-ionic dyes used for hydrophobic fibres like polyester and cellulose acetate, their typical molecular structure is shown in Figure I-16. The volatility of disperse dyes allows their vapors to be effectively absorbed by these fibres. Also known as dispersible or plasto soluble dyes, they are applied as finely dispersed powders in dye baths.

These dyes are stable at high temperatures, which allow diffusion into synthetic fibres before fixation. Widely used in dyeing manufactured fibres, particularly polyester and polyamide, they require a dispersing agent for effective application [15, 16].

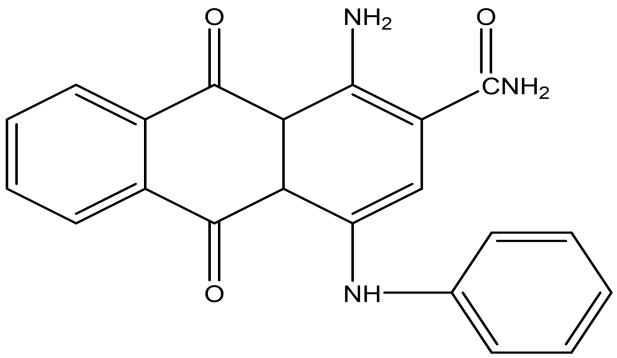

Figure I- 16: Structure of disperse blue 6.

I.2.5. Toxicity of dyes

Not all synthetic dyes are harmful, for example some fiber-reactive dyes can bond to fibers like cotton and rayon without the need for toxic mordants. The toxic property of a dye more rely on its chemical structure than the dyeing process itself [17]. Dyes with heavy metals and those that lead to cancer are especially harmful. Very reactive dyes, acid dyes, and disperse dyes can be highly toxic to the skin.

Currently, every year 0.7 million tons synthetic dyes produced, 12% of which are released into the environment [18]among these, azo and cationic dyes are among the most toxic and are associated with health issues such as cancer and allergies.

Natural dyes are less toxic than the synthetic dyes which can pollute the water, which will affect the aquatic ecosystems and human health. Basic dyes can damage the algae, and the azo dyes used in textile industry causes several risks to humans such as cancer.

However, it is important to reduce the presence of those dyes in the environment and making sure to treat the waste water to breaking them down.

Part 3:

Treatment methods

I.3. Treatment methods

I.3.1. Adsorption

I.3.1.1. Introduction

Since the beginning of the 20th century, adsorption has garnered a lot of scientific attention because of its numerous industrial, environmental and biological uses. The term adsorption was first proposed by Kayser in 1881 [19].

Adsorption is an essential step in many catalytic processes and is widely used to separate components in both laboratory and industrial environments. In addition, it has an essential role in purifying water, air and soil. Adsorption is a process in which molecules from a fluid whether a gas or a liquid attach themselves to the surface of a solid. The molecules that become attached are referred to as the 'adsorbate', while the solid hosting them is known as the 'adsorbent'. This surface includes not only the exterior of the solid but also its intricate internal landscape, composed of pores and cavities that offer abundant sites for molecular attachment.

I.3.1.2. Types of adsorption

According to the type of interaction established between the adsorbate and the adsorbent, two types of adsorption are considered, physical and chemical [20].

a- Physical adsorption

Physical adsorption occurs through weak forces such as Van der Waals bonds, electrostatic interactions, dipole-dipole and hydrogen bonds, among others, this process is reversible [20]and not very specific, the strength of the interactions involved can be estimated by the adsorption energy which is between 5 and 40 kJ/mol which considered weak so desorption can therefore be total [21].

The physical adsorption can be in in monolayer or multilayer.

b- Chemical adsorption

The adsorbate bonds chemically with the adsorbent surface, which makes this interaction irreversible, very specific [20]. The adsorption energy is greater than 80 kJ/mol so the desorption is difficult. The chemical adsorption is generally monolayer because the presence of valence bonds between the adsorbate and the adsorbent excludes the possibility of multilayer [21].

I.3.1.3. Mechanism of adsorption

The process of adsorption unfolds through a series of distinct stages, as outlined below:

- ✓ **Diffusion from bulk solution:** The adsorbate molecules move from the bulk liquid phase near to the adsorbent surface.

- ✓ **Film diffusion:** The molecules diffuse through the liquid film to the surface of the grains.
- ✓ **Pore diffusion:** The phenomenon continues with the transfer of the adsorbate in the porous structure to the active sites.
- ✓ **Adsorption:** Finally, the adsorbate attaches to the active sites on either the internal or external surfaces of the adsorbent through physical interactions such as Van der Waals forces or hydrogen bonding or through the formation of chemical bonds, whether ionic or covalent [22].

I.3.1.4. Main factors influencing adsorption

Many factors can affect the adsorption of a substance on an adsorbent material [23], among the most important we found:

a. Temperature

The physical adsorption is generally an exothermic process, which make its development is favoured at low temperature [23].

On the other side, the chemical adsorption is endothermic so it prefers high temperature.

b. pH of the solution

One of the most important factors affecting adsorption capacity is the pH, the variation in pH cause a variation in the degree of ionization of the adsorbed molecule and in the surface properties of the adsorbent [24].

In general, the initial pH value can increase or decrease the adsorption rate [24].

c. The initial dye concentration

The initial concentration has a significant effect on the adsorption, generally with the increasment of this concentration dye adsorption diminue as the active sites on the adsorbent surface become saturated. Conversely, increasing the initial dye concentration enhances the adsorption capacity, likely due to the greater driving force for mass transfer at higher concentrations [24].

d. The solubility of the adsorbate

The adsorption increase when the solubility of the substance in the solvent decrease [25].

e. The nature of the adsorbent

Adsorption is characterized by its high selectivity, which means that an adsorbent prefer to adsorbs certain substances over others [25].

I.3.1.5. The adsorption isotherm

The adsorption process can be described using an adsorption isotherm. An isotherm is a curve that represents the relationship between the amount of solute adsorbed Q_e (mg/g) and the

concentration of solute in solution C_e (mg/L) [26]. They help in determining the optimum adsorption capacity of adsorbent and indicate the efficiency of the adsorbent, and also allows an estimation of the validity of adsorbent's application [27].

According to Giles et al there is four classes for those isotherms named S (Sigmoidal), L(Langmuir), H (High affinity) and C (constant partition) as seen in Figure I-17 [23]:

Type S: Are obtained when the solute molecules only attach to the solid through a single group [29].

Type L: The most common, indicates the flat adsorption of bifunctional molecules [26].

Type H: Starts from a positive value but not from zero, indicates high affinity which means the adsorption is complete at low concentrations [26].

Type C: Are in the form of a straight line, this type of curve is obtained when there is competition between the solvent and the solute to occupy the sites of the adsorbent [19].

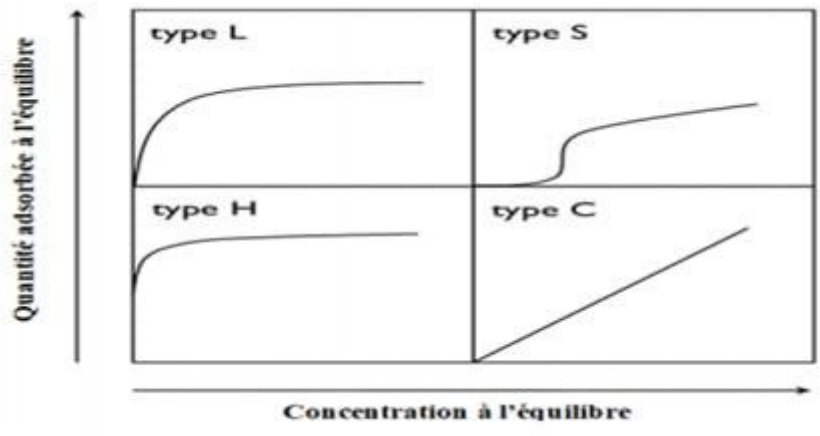

Figure I- 17: The types of adsorption isotherms according to (Giles et al) [23].

I.3.1.6. Modeling of adsorption isotherms

Many theoretical models are proposed to describe the relation between the mass of adsorbate fixed at equilibrium (Q_e) and the concentration under which the reaction takes place (C_e) [26]. The mass of adsorbate fixed at equilibrium is given by the following equation:

$$Q_e = \frac{(C_0 - C_e)}{m} \times V \qquad (1)$$

C_0: Initial concentration of the adsorbate (mg/L).

C_e: Equilibrium concentration of the adsorbate (mg/L).

V: Volume of the solution (L).

m: Mass of adsorbent (g).

a. Langmuir's isotherm

The Langmuir's isotherm (Langmuir,1918) allows the determination of the maximum adsorption capacity of the adsorbent material and the rate constant of the adsorption process [24].

This model operates under the following set of assumptions:

- ✓ The adsorbent has a limited adsorption capacity (Q_{max}).
- ✓ All the active sites are identical, and the adsorption is monolayer.
- ✓ There are no interactions between the adsorbed molecules [23].

The non-linear equation of Langmuir is:

$$Q_e = \frac{Q_{max} \times K_L \times C_e}{1 + K_L \times C_e} \quad (2)$$

K_L: The Langmuir equilibrium adsorption constant (L/mg).

C_e: The concentration of adsorbate in solution at equilibrium (mg/L).

Q_{max}: The maximum Langmuir saturation adsorption capacity (mg/g).

Q_e: The adsorption capacity of the adsorbent at equilibrium (mg/g).

b. Freundlich isotherm

Freundlich model (Freundlich, 1906) is a model that applies to many cases, particularly in the case of multilayer adsorption with possible interactions between adsorbed molecules [23].

The nonlinear expression of Freundlich equation is:

$$Q_e = K_F \times C_e^{\frac{1}{n}} \quad (3)$$

K_F : Freundlich constant indicating adsorption capacity.

$\frac{1}{n}$: Adsorption intensity.

c. Temkin isotherm

According to the Temkin isotherm, the heat of adsorption should decrease linearly with adsorption coverage on the adsorbent due to interactions of adsorbent and adsorbate [27].

The nonlinear equation is:

$$Q_e = \frac{R \times T}{b_T} \mathrm{Ln}(K_T C_e) \quad (4)$$

K_T and b_T: Are Temkin isotherm constants.

R: Gas constant (8, 31 $J.mol^{-1}.K^{-1}$).

T: Temperature (K).

I.3.1.7. Adsorption kinetic

Describes the rate at which a contaminant (adsorbed) binds or is released from an aqueous solution to the surface of a solid (adsorbent). It is an important factor in evaluating the performance of materials used in water purification.

Mathematical models, either linear or nonlinear are used to analyze adsorption behaviour. The best model is determined using goodness-of-fit indices (GFIs) to accurately represent the process.

By studying kinetics, it is possible to:

- ✓ Estimate the amount of contaminant adsorbed over time.
- ✓ Understand the adsorption mechanism.
- ✓ Understand how the contaminant transitions from the liquid phase to the solid phase [26, 27].

I.3.1.8. Modeling of adsorption kinetics

a. Pseudo first order (Largergren model)

This model states that the difference in the concentration and rate of adsorbate removal over time is directly proportional to the rate of change in adsorbate uptake at a given reaction time. Also known as Lagergren model, it is often employed to characterize the initial phase of the adsorption process, the model is expressed through the following equation [27, 28]:

$$\frac{dq_t}{dt} = K_1(q_e - q_t) \quad (5)$$

$\frac{dqt}{dt}$**:** Adsorption rate at time t.

$\mathbf{q_e}$**:** Quantity of adsorbate at equilibrium (mg/g).

$\mathbf{q_t}$**:** Quantity of adsorbate at time t (mg/g).

$\mathbf{K_1}$**:** Pseudo-first-order rate constant (min^{-1}).

Through the integration of this equation, we obtain the following equation:

$$q_t = q_e(1 - e^{-K_1 t}) \quad (6)$$

b. Pseudo-second order

In pseudo-second order kinetics, adsorption occurs on two surface sites (referred to as "Blanchard's model" by certain writers) and Thus, the following second-order differential equation can be used to express it [28].

$$\frac{dq_t}{dt} = K_2(q_e - q_t)^2 \quad (7)$$

$\frac{dqt}{dt}$**:** Adsorption rate at time t.

$\mathbf{q_e}$**:** quantity of adsorbate at equilibrium (mg/g).

$\mathbf{q_t}$**:** quantity of adsorbate at time t (mg/g).

$\mathbf{K_2}$**:** pseudo-second-order rate constant (min^{-1}).

Integrating this equation, we obtain:

$$\frac{dq_t}{dt} = K_2(q_e - q_t)^2 \quad (8)$$

c. Elovich kinetic model

Mainly study of chemical adsorption on highly heterogeneous adsorbents and study of the Elovich equation is often employed to describe the kinetics of gas adsorption on solid surfaces, as well as the adsorption of pollutants from aqueous solutions [23, 28].

$$\frac{dq}{dt} = \alpha e^{(\beta q_t)} \quad (9)$$

The equation can be written in its nonlinear form as follows:

$$q_t = \frac{1}{\beta} Ln(1 + \alpha\beta t) \quad (10)$$

$\boldsymbol{\alpha}$**:** The initial adsorption rate in (mg/g.min).

$\boldsymbol{\beta}$ **:** The desorption constant (mg/g) reflects both the degree of surface coverage and the activation energy associated with chemisorption.

d. Intraparticle diffusion (IPD)

The diffusion model is based on Fick's second law, which explains how solutes move within an absorbent particle and controls the rate of adsorption. There are several types of diffusion, one of the most important was Intraparticle diffusion, which refers to the movement of molecules within the absorbent particles, but not just across the outer surface [29].

$$q_t = K_{id}^{0.5} + C \quad (11)$$

$\mathbf{q_t}$**:** The adsorption capacity at time t (mg/g).

$\mathbf{K_{id}}$**:** The intraparticle diffusion rate constant.

C: A constant related to the boundary layer thickness.

I.3.1.9. Models analysis

To determine which model fits better in both the adsorption isotherm and the kinetic, three different values are considerable:

- ✓ The coefficient of determination (R^2).

- ✓ The Root Mean Square Error:

$$\text{RMSE}\ (\%) = \sqrt{\frac{\sum_{i=1}^{N} (Q_{cal} - Q_{exp})^2}{N}} \quad (12)$$

- ✓ The Chi-Square:

$$x^2 = \sum_{i=1}^{N} \left[\frac{(Q_{exp} - Q_{cal})^2}{Q_{cal}}\right] \quad (13)$$

The most suitable model is the one that minimizes RMSE and χ^2 values while achieving an R^2 value closest to one.

I.3.2. Photocatalysis

I.3.2.1. Introduction

The photocatalytic process was discovered by scientist Edmond in 1839 from natural photosynthesis. In natural photosynthesis, plants, microalgae, and a few microscopic organisms collect energy from sunlight that helps in transformation of CO_2 and H_2O to carbohydrate, solar energy can be converted into the forms of heat and electricity directly and can further be utilized for different applications [30].

They received wider attention after Fujishima and Honda discovered that water can be photo-electrochemically decomposed into hydrogen and oxygen using a semiconductor (TiO_2) electrode under UV irradiation [31, 32], since its emergence, heterogeneous photocatalysis has captivated the scientific community, thanks to its vast potential across diverse applications.

The word "photocatalysis" is comprised of two parts: the prefix "photo", which means "light", and "catalysis", which refers to the process of accelerating a chemical reaction through a catalyst without the catalyst itself being consumed in the process. In natural photosynthesis, organisms such as plants, microalgae, and certain microorganisms absorb sunlight to convert CO_2 and H_2O into carbohydrates. This process inspired the development of photocatalytic technologies that harness solar energy, which can be transformed into heat or electricity for various applications. Given the challenges related to energy harvesting, storage, and the intermittent nature of sunlight, recent advances in photocatalysis aim to address these issues and meet the increasing global demand for energy.

We have two types of Photocatalysis:

- ✓ Homogeneous Photocatalysis: The reactants and the catalyst exist in the same phase (e.g., dissolved transition metal complexes and ozone reactions).
- ✓ Heterogeneous Photocatalysis: The catalyst is in a solid phase, while the reactants are in a liquid or gaseous phase. This type is commonly employed in environmental fields, particularly in the treatment of wastewater and the purification of air [30].

I.3.2.2. Fundamental Mechanism

Photocatalysis is a process where light energy is used to activate a semiconductor material, leading to redox reactions that can degrade pollutants. The mechanism underlying this process unfolds through several distinct steps:

- ✓ When a semiconductor photocatalyst (e.g., TiO_2, ZnO) absorbs photons with energy equal to or greater than its bandgap(energy required to promote an electron), an electron (e^-) becomes excited from the valence band to the conduction band, leaving behind a positively charged hole (h^+) in the valence band [31].

$$\text{Semiconductor} + h\nu \rightarrow e^- + h$$

- ✓ The generated electrons and holes may either migrate to the surface of the photocatalyst or undergo recombination a process that dissipates energy as heat and diminishes the overall photocatalytic efficiency [31].

$$e^- + h^+ \rightarrow \text{heat}$$

- ✓ If they reach the surface without recombining, they participate in redox reactions:
  - ➢ Acting as oxidizing agents, the holes (h^+) interact with water molecules to generate hydroxyl radicals (•OH), which are intensely reactive and play a crucial role in degrading pollutants [32].

$$h^+ + H_2O \rightarrow \cdot OH + H^+$$

  - ➢ The electrons (e^-) can reduce oxygen molecule to form super oxide radical ($\cdot O_2^-$) [11, 14].

$$e^- + O_2 \rightarrow \cdot O_2^-$$

- ✓ The reactive species generated such as hydroxyl and superoxide radicals decompose pollutants into benign end products like CO_2 and H_2O [33].

$$\cdot O_2^- + \cdot OH + \text{pollutant} \rightarrow CO_2 + H_2O + \text{degraded products}$$

The degradation of pollutants follows five major steps. In steps 1 and 2, pollutant molecules are transferred to the surface of the photocatalyst and followed by adsorption onto the active sites. In step 3, once the pollutants get attached to the active sites, the electrons get photo excited and initiate the photocatalytic degradation process. In steps 4 and 5, once the pollutant is degraded, desorption occurs, and finally, the degraded molecules are released to the water surface [34]. The general mechanism of heterogeneous photocatalysis is summarized in Figure I-18.

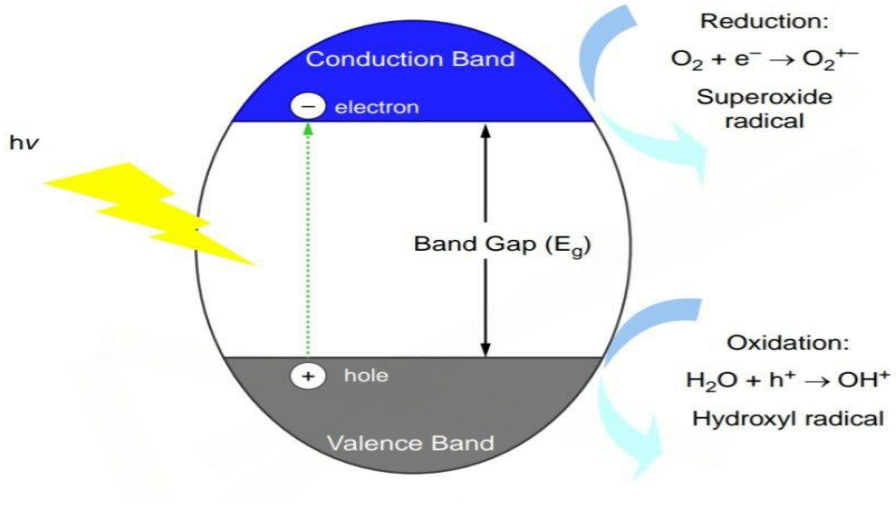

Figure I- 18: Mechanism of photocatalysis process[30].

I.3.2.3. Semiconductors

Oxide-based semiconductors are the most used in photocatalytic applications because of their excellent light absorption, charge-transfer properties, and electronic structure. These materials characterized by their small band gaps (energy needed to move from the valence band to the conduction band), that allow them to function as both charge-generating and light-absorbing components.

A wide range semiconductor materials, including ZnO, TiO_2, CdS, WO_3, Cu_2O, ZnS, ZrO_2, CeO_2, SnO_2 and $SrTiO_3$, have been used as photocatalysis due to their stability, narrow band gaps, strong solar radiation response, and well-defined electronic structures.

In recent years, researchers have been investigating new materials to improve solar energy utilization. Over the past decade, significant efforts devoted to developing visible-light-active (VL) photocatalysts for wastewater treatment. At this time, more than 150 semiconductor materials including hydroxides, oxides have been explored for the purification of environmental systems.

For effective photocatalysis, a photocatalyst must efficiently transfer charge carriers to the semiconductor-electrolyte interface. Although many binary compounds exhibit semiconducting properties, not all of them are suitable for photocatalytic applications [35].

I.3.2.4. Factors affecting the photocatalysis process

a. pH effect

pH is one of the most influential factors on both the adsorption and the photocatalysis processes [36].

The pH level in photocatalysis plays a crucial role in altering the surface charge of the photocatalyst as well as affecting the characteristics of the organic pollutant.

When we use the TiO_2 as photocatalyst the Ph_{PZC} is around 6 - 6.5, and at pH < pH_{PZC} the surface of the photocatalyst is charged positively which enhance the adsorption of anions, and at pH >pH_{PZC} it charged negatively it enhance the adsorption of cations and when the pH is near to Ph_{PZC} it favorise the phenomenon aggregation and formation of TiO_2 clusters [36].

This charge variation affect the interaction between the photocatalyst and the pollutant and The formation of hydroxyls radicals(•OH) (a highly reactive species responsible for breaking down pollutants)which is higher in basic pH [33].

Finally the optimal pH depends the nature of the pollutant, some compounds degrade more efficiently in neutral or acidic environments [37].

b. The concentration of the pollutant

The concentration of the pollutant plays a significant role in the efficiency of the photocatalysis process.

When the concentration of the pollutant increase the degradation efficiency decrease due to more polluants molecules interact with the active site in the surface of the photocatalyist, this reduces the number of photons reaching the surface, thereby diminishing the generation of hydroxyl radicals (•OH), which are vital to the degradation process.

c. Effect of catalyst concentration

The concentration of the catalyst is an important parameter, it can affect the degradation rate process. The initial degradation rate of organic substances is directly proportional to the catalyst concentration (TiO_2) at low concentrations. However, beyond a certain point, the concentration becomes independent of the catalyst concentration. An optimum is reached when TiO_2 fully absorbs the photons. Although higher catalyst concentrations provide more active sites, they may paradoxically reduce the pollutant's degradation efficiency, by blocking the light source. Reducing photon penetration in the surface of the catalyst [36, 37].

d. The temperature effect

Temperature is an important environmental factor, the photocatalytic system does not require heat input because it is a photon activation process. Most photoreactions are not sensitive to temperature changes, such that when the temperature decreases, adsorption is enhanced, which is an exothermic phenomenon. However, when the temperature increases, the thermal adsorption of pollutants becomes weaker [36, 37].

e. The time effect

The time have a significant effect on the degradation efficiency of the pollutant, however this process should be rapid and efficient.

In previous studies they found that the time should vary from 15 to 330 min, that lead to a degradation percentages vary from 10% to 100%, depending on the photocatalyst, the dye type, and experimental conditions [33].

I.3.2.5. Advantages and disadvantages of photocatalysis

A. Advantages

- ✓ The photocatalysis does not need a complex equipment its only need water, a photocatalyst, and a light source.
- ✓ The reaction is eco-friendly and does not generate a harmful by-product.
- ✓ It can work in normal conditions without requiring high temperature or pressure.
- ✓ The photocatalysis used are non-toxic, and do not generate hazardous by-products.

B. Disadvantages

- ✓ Some photocatalysts degrade over time, especially under UV radiation.
- ✓ Most photocatalyst absorbs the UV light only which limits the efficiency under the sunlight.
- ✓ Necessary recovery of photocatalyst after reaction.

Chapter II

Experimental Part

II. Experimental part

II.1.Introduction

In this chapter, we discuss the physical and chemical properties of Congo Red and the waste foundry sand. We also present all the methods used to study the adsorption and photocatalysis of Congo Red by WFS.

We also present the materials and products used, as well as the protocol to follow in this study.

II.2. Objective

The objective is to study the efficiency of the WFS as an adsorbent of the Congo Red dye and to study the effect of key factors, including pH, concentration and temperature, on its performance.

We also intend to study the photocatalysis process to compare these two methods.

II.3. Materials and methods

II.3.1. Equipment Used

We used the following equipment for our work:

Figure II- 1: SpectrophotometerUV (UV iLine 9400C).

Figure II- 2: pH meter

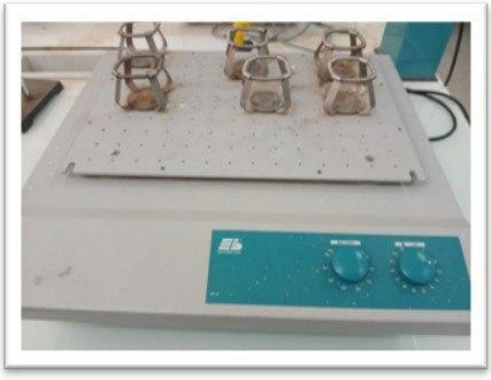

Figure II- 3: Agitation mechanism.

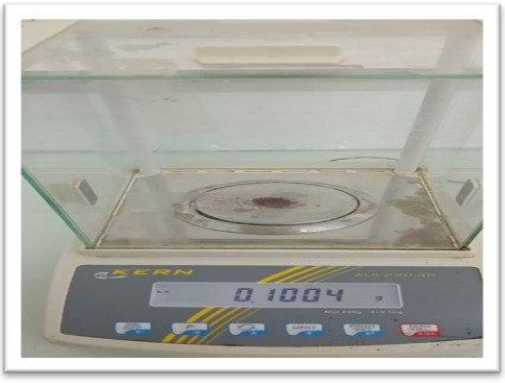

Figure II- 4: Analytical balance.

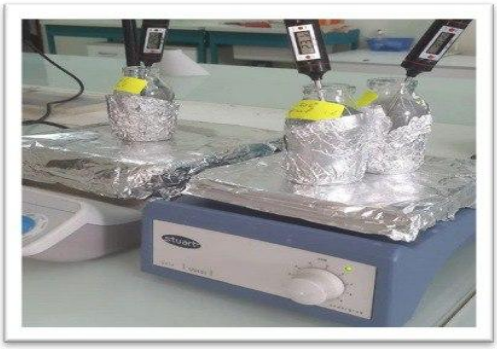

Figure II- 5: Magnetic stirrer.

Figure II- 6: UV light room.

II.3.2. Products

II.3.2.1. Waste foundry sand

The waste foundry sand used in the experimental study was obtained from Turkey. It was used as foundry sand in the metal casting industry. After the casting process, the sand becomes contaminated with residues from metals and binders; this makes it unsuitable for further use.

The chemical compositions of foundry sand are given on Table II-1 below:

Table II- 1: Major components of the WFS

Major components	Wt(%)
Al_2O_3	60
SiO_2	35
Fe_2O_3	3
TiO_2	2

II.3.2.2. Congo Red

Congo Red belongs to the class of anionic acid dyes with well-known similar physical and chemical properties. It has a molecular formula of $C_{32}H_{22}N_6Na_2O_6S_2$ and a hydrophobic center composed of two phenyl bonds via a biphenyl bond, giving it a linear molecular nature. The dye is fluorescent and easily detectable by spectroscopic techniques. It has high solubility in water. Despite its toxicity and limited industrial use, it is widely used as a sensitive pH indicator and in histology and mycology applications due to its stable physical and chemical properties. The main physico-chemical properties of Congo Red are summarized in Table II-2.

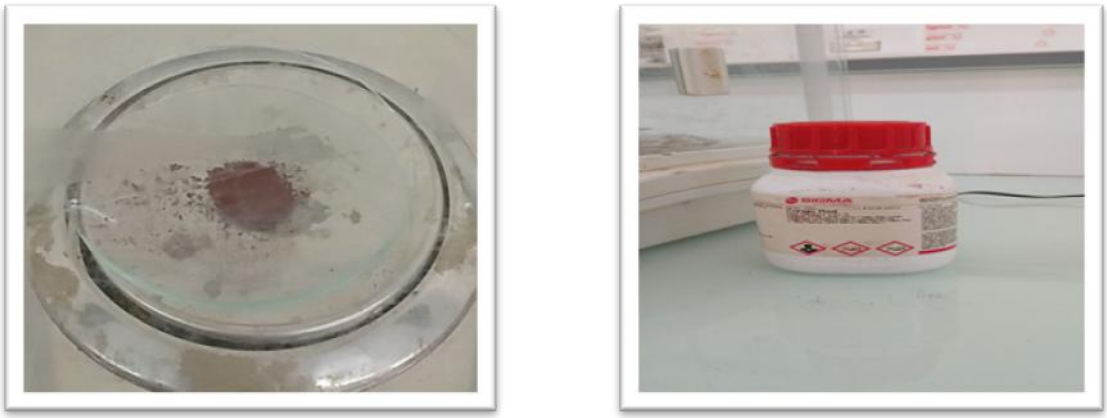

Figure II- 7: Congo Red dye

Table II- 2: Some physico-chemical characteristics of RC dye

Dye	Congo Red
Chemical formula	$C_{32}H_{22}N_6Na_2O_6S_2$
Type	Anionic
Molar mass (g/mol)	696.66 g/mol
Solubility in water	High solubility
Wavelength	500 nm
Structure	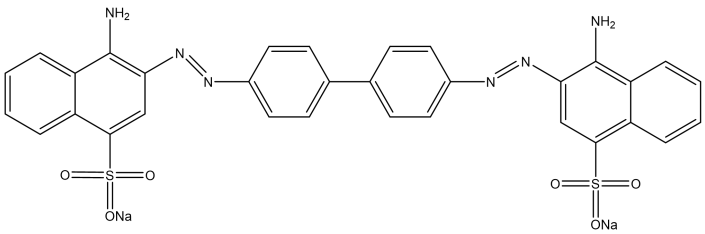

II.4. Characterisation of the WFS

II.4.1. Infrared spectroscopy (FTIR)

Infrared spectroscopy is a widely used technique for the identification of the species present on the surface of solids [19], those groups forms the adsorbent-adsorbate bonds.

This technique is based on the absorption of infrared radiation by the sample and the measurement of the quantity of light absorbed, as a function of the wavelength [38], the infrared domain is from 400 cm^{-1} to 4000 cm^{-1}.

II.4.2. X-ray diffraction (XRD)

X-ray diffraction is a technique that allows us to determine the crystal structure of a material analyzing the pattern generated when X-rays interact with its crystal lattice. Each phase

produces a unique pattern, and factors such as defects, the results can be affected by microstrains and crystal size.

XRD is useful for determining the type and quantity of crystalline phases [1, 39].

II.4.3. Boehm titration

This method is employed for the identification and quantification of surface functionalities of the WFS. To accomplish this, we followed the steps outlined below:

- ✓ First we started by preparing the solutions of NaOH , Na_2HCO_3 , Na_2CO_3 and HCl with C=0,05 M.
- ✓ Then we put 25 ml of each solution in a beaker and add on them a 0, 25 g of the adsorbent (WFS) and let them agitate for 24 h.
- ✓ After the 24 h the solutions were filtered.
- ✓ After that, 6 mL of each solution (Na_2HCO_3, Na_2CO_3, NaOH) were titered by the HCl and Phenolphthalein as a coloured indicator to determine the acid functions, and for the basic functions the HCl was titered by the NaOH.
- ✓ Finally, we repeated the titration 4 times to ensure the results.

II.4.4. pH point of zero charge (pH_{PZC})

- ✓ In this experiment, we prepared a KNO_3 solution with 0.1 M.
- ✓ The volume of 50 ml was then divided into nine flasks.
- ✓ The pH was then adjusted using a pH meter, thus obtaining the initial pH.
- ✓ Then, a 0.1 g mass of WFS was weighed and added to each solution. The solutions were then shaken at 200 rpm for half an hour.
- ✓ After half an hour, the liquid was filtered and the pH of each solution was measured. This resulted in the final pH.
- ✓ Then, we plotted the pH_f - pH_i curve in terms of pH_i.

II.5. Preparation of Congo red solutions

- **Stock solution**

  To carry out our different experiments, a stock solution of Congo Red was prepared, with a mass concentration of 100 mg/L and 1 L volume. To achieve this, an electronic balance is used to measure 0.1 g of Congo Red, then this amount is dissolved in a 1 L volumetric flask using distilled water as the solvent.

- **Diluted solutions**

A series of calibration solutions at concentrations of (5, 10, 20, 30, and 40 mg/L) were formulated by diluting the stock solution, following the dilution law below:

$$C_1 \times V_1 = C_2 \times V_2 \quad (14)$$

C_1: Concentration of the stock solution (mg/L).

V_1: Volume of the stock solution (mL).

C_2: Concentration of the diluted solution (mg/L).

V_2: Volume of the diluted solution (mL).

II.6. Calibration curve

The calibrations solutions presented in Figure II-8 were analyzed using UV-visible spectrophotometer. The maximum absorption wavelength was determined by scanning between 400 and 800 nm, We measured that λ=500 nm, and then it was used to measure the absorbance of the dye at different concentrations.

The unknown concentrations of Congo Red can be determined using the calibration curve A= f (C) , using beer lambert equation :

$$A = \varepsilon . l . c \quad (15)$$

A: Absorbance of the solution.

ε: Specific extinction coefficient of the solute ($L.mol^{-1}.cm^{-1}$).

l: Thickness of the optical cell (cm).

C: Concentration of the solution (mol/L).

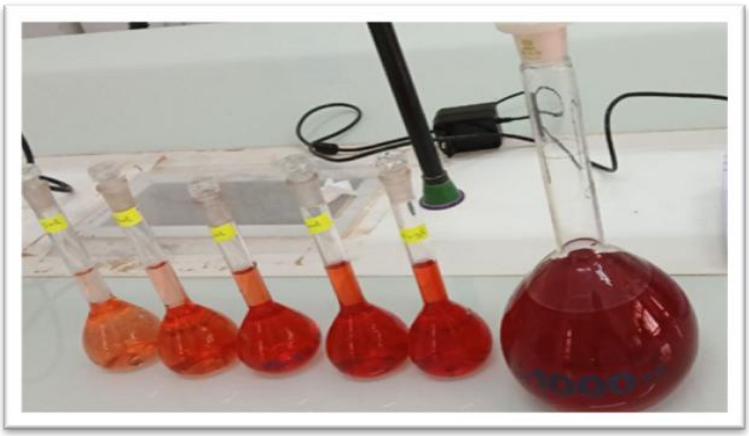

Figure II- 8: Calibrations solutions.

II.7. Batch adsorption

The experiments were performed by interacting various concentrations of dye (10-30 mg/L) solutions and volume of 30 ml mixed with a known amount of waste foundry sand at an adjusted pH in a rotary shaker at an ambient temperature and 200 rpm for 60 min to attain equilibrium. The samples were filtered. Then the absorbance was determined at λ_{max}= 500 nm

using a UV-vis spectrophotometer (UV iLine 9400C) the adsorption capacity and yield of adsorption were calculated by applying equations (15) and (16), respectively:

$$Q_e = \frac{(C_0 - C_e)}{m} \times V \quad (16)$$

$$\text{yeild}\% = \frac{(C_0 - C_e)}{C_0} \times 100 \quad (17)$$

II.8. Study of the adsorption of Congo Red by Waste foundry sand

The Box Behnken design (BBD) was used to determine the number of experiments to be carried out to evaluate the possible interactions between studied parameters and their effects on the adsorption of the Congo red dye [40]. Literature showed that the importance of using BBD is found to be very effective for optimizing the adsorption influencing factors [41].

Three process-influencing parameters (the WFS mass, pH of the solution, initial dye concentration) were examined for the Congo red adsorption investigation. The equilibrium period, or 60 minutes, was set as the contact time between the adsorbent (RC–WFS) and the adsorbate.

Software called Design Expert 11 was used to do statistical analysis. One benefit of this method is that it does not require tests in harsh environments or combinations in which all elements are simultaneously set to their maximum or minimum levels. 15 run were generated by design expert software to study the effect of the three parameters.

As indicated in Table II-3, the independent variables were analyzed at three different levels: low (-1), center (0), and high (+1).

Table II- 3: Experimental levels of the variables.

	A	B	C
	WFS mass (mg)	C_0 (mg/L)	pH
-1	20	10	2
0	30	20	6
1	40	30	10

Table II- 4: Box Behnken design.

	A	B	C
1	-1	-1	0
2	1	-1	0
3	-1	1	0
4	1	1	0
5	-1	0	-1
6	1	0	-1
7	-1	0	1
8	1	0	1
9	0	-1	-1
10	0	1	-1
11	0	-1	1
12	0	1	1
13	0	0	0
14	0	0	0
15	0	0	0

II.9. Regression model

The data were analyzed using ANOVA to develop a predictive quadratic model, which describes the relationship between the input factors (x_1, x_2, ..., x_3) and the response to be studied.

$$Y = a_0 + a_1X_1 + a_2X_2 + a_3X_3 + a_1\,^2X_1\,^2 + a_2\,^2X_2\,^2 + a_3\,^2X_3\,^2 + a_1a_2X_1X_2 + a_1a_3X_1X_3 + a_2a_3X_2X_3$$

Y: the calculated answer.

α_0 : the y-intercept.

α_1, α_2, and **α_3:** linear coefficients.

$\alpha_1\,\alpha_1$, $\alpha_2\,\alpha_2$, $\alpha_3\,\alpha_3$: quadratic coefficients.

$\alpha_1\,\alpha_2$, $\alpha_1\,\alpha_3$, $\alpha_2\,\alpha_3$: interactive coefficients.

II.10. Kinetic study

The experiment was conducted on an optimum solution, after preparation, the series of vials were placed in a special device known as a shaking mechanism, where they were processed at an ambient temperature, with agitation of 200 tr/min.

The shaking process continued for specific periods of time: 5, 10, 15, 30, 45, and 60 minutes. After the shaking process was completed, the used soil was separated from the solutions by filtration.

The resulting solutions were analyzed using a UV-Vis spectrophotometer at a wavelength of 500 nm.

The obtained absorbance values allowed us to plot the kinetics curve by calculating the equilibrium concentration (C_e) using the Beer-Lambert law, as well as the equilibrium absorbed quantity (q_e) at different concentrations.

II.11. Adsorption isotherm

We conducted an experiment on an optimal solution, as the solutions had varying concentrations (5, 10, 20, 30, 40 mg/L). The tubes containing the solutions were subjected to a continuous stirring process using a shaking device at a speed of 200 rpm for 60 minutes. After the stirring period ended, the solutions were filtered to isolate the solid material and then the filtrate was subjected to analysis using ultraviolet-visible (UV-Vis) spectrophotometer at a wavelength of 500 nm.

II.12. Temperature effect

The effect of temperature on the optimum solution was studied. The required temperatures were adjusted using a magnetic stirrer equipped with a thermometer at three range temperatures: 20, 30, and 40 °C as shown in Fiure II-9.

After reaching the specified temperature, the solutions were filtered to separate the solid. The filtrate was then analyzed using UV–Vis spectrophotometer.

Figure II- 9: Magnetic stirrer with termometer.

II.13. Thermodynamic study

After studied the temperature effect on the adsorption of CR on WFS. The thermodynamic parameters (the standard Gibbs free energy change (ΔG^o). The standard enthalpy change (ΔH^o) and the standard entropy change (ΔS^o), that characterize the equilibrium state of a system are

calculated. These parameters were determined to evaluate the feasibility, spontaneity and the nature of the interaction involved in the adsorption process [42].

$$\Delta G° = - RTLn(K_C) \quad (18)$$

$$Ln(K_C) = \frac{\Delta S°}{R} - \frac{\Delta H°}{RT} \quad (19)$$

$$\Delta G° = \Delta H° - T\,\Delta S° \quad (20)$$

Kc: Is $\frac{Qe}{Ce}$.

ΔG °, ΔH° and **ΔS°**: Are change in Gibbs free energy (kJ/mol), enthalpy (kJ/mol) and entropy (kJ/mol. K) of adsorption, respectively.

R: The universal gas constant (8.314 J/K/ mol).

T: The temperature (K).

II.14. Photocatalysis treatment

A 20 mL solution is made in a beaker, once the pH is set to 2, a mass of WFS is added. The solution is kept homogenous with the help of a magnetic stirrer and an external UV lamp. A vessel contains the reactor, stirrer and lamp as presented in Figure II-10. Samples are collected, filtered, and examined using a UV-Vis spectrophotometer (model UV iLine 9400C) at intervals of 5, 10, 15, 30, 45, and 60 minutes.

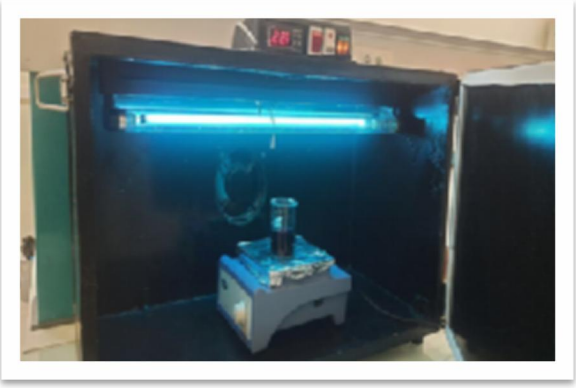

Figure II- 10: Photocatalysis equipment.

Chapter III

Results and Discussion

III. Results and discussion

III.1. Characterisation of the WFS

III.1.1. Infrared spectroscopy (FTIR)

The FTIR spectra of the WFS before and after the CR adsorption using fourier transform infrared spectrophotometer in the region of 400-4000 cm^{-1} (FTIR.Perkin-Elmer Spectrum 400). are presented in Figure III-1 below:

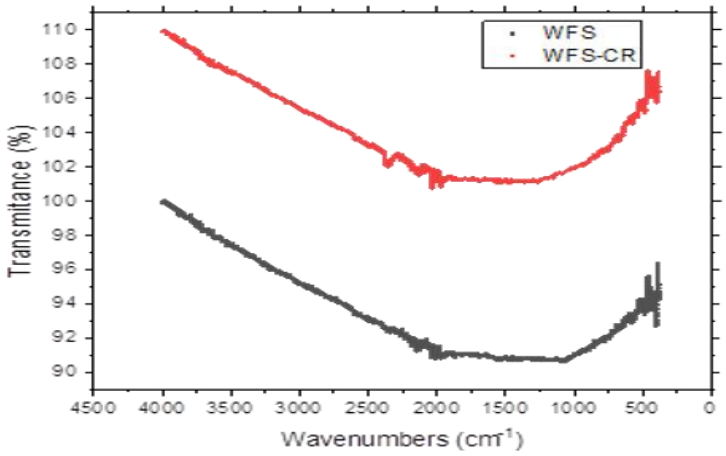

Figure III- 1: Infra-red spectroscopy of the WFS.

The Table III-1 present the interpretation of these results:

Table III- 1: FTIR Analysis of WFS and WFS-CR.

WFS		
Band position (cm^{-1})		Suggested assignments
Before adsorption	After adsorption	
2335.15	2358.96	Nitrile group C≡N
2004.98	2031.97	Metal carbonyl M(CO)
627.99	671.50	Carbon-halogen C-X
494.26	486.91	Silicon-oxygen Si-O
434.55	439.18	Metal-halogen M-X

The FTIR analysis of WFS in this study revealed some differences compared to previously reported spectra [43]. These variations may be attributed to differences in the source of the sand, foundry processes, or impurities present in the sample.

III.1.2. X-ray diffraction (XRD)

The crystal structure of the waste foundry sand was determined by "X-ray diffractometer, XRD" (XRD Rigaka Dmax-Rapid II), This analysis aims to identify the composition of WFS and its composition.

The results are shown in Figure III-2. It is clear that there ar obvious peaks at 2θ values of 27, 36, 42, 57 refers to Al_2O_3, at 17, 26, 33 refers to Fe_2O_3, at 21, 28, 66 for SiO_2 and other peaks at 41, 54, 67 refers to TiO_2.

These compounds are commonly found in industrial waste like WFS, suggesting that the material is a good adsorbent and effective for photocatalytic treatment [44].

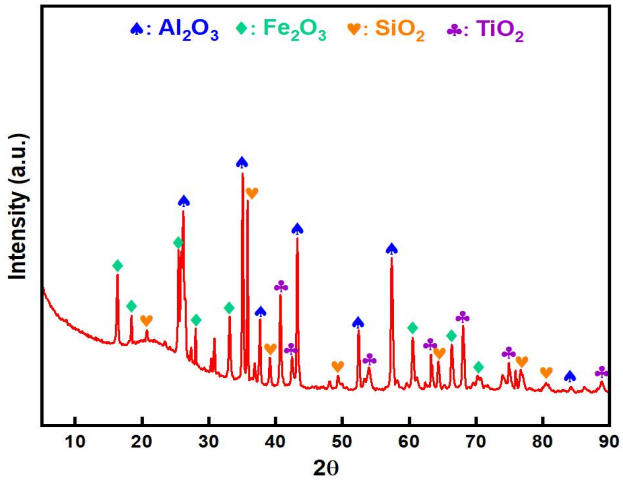

Figure III- 2: X-ray diffraction of the WFS.

III.1.3. Boehm titration

The Boehm titration was carried out to determine the surface functional groups present on the WFS. The measured values obtained from this analysis are compiled in Table III-2. This table provides the amounts of the different acidic and basic groups identified on the surface of the material.

Table III- 2: Boehm titration results.

Adsorbent	Phenol groups(mmol/g)	Carboxylic groups (mmol/g)	Acidic sites	Basic sites
WFS	2.29	4.85	7.14	4.05

The Boehm dosage results showed that Waste foundry sand (WFS) contains a greater number of acidic sites (7.14 mmol/g) compared to basic sites (4.05 mmol/g).

This abundance of acidic sites improved the interaction with anionic dyes like CR.

III.1.4. pH of pint zero charge (pH_{PZC})

To evaluate the surface charge characteristics of WFS, the point of zero charge (pH_{PZC}) was determined. Figure III-3 illustrates the relationship between the change in pH (pHf - pHi) and the initial pH of the solution. The intersection point indicates the pH at which the surface of the material carries no charge.

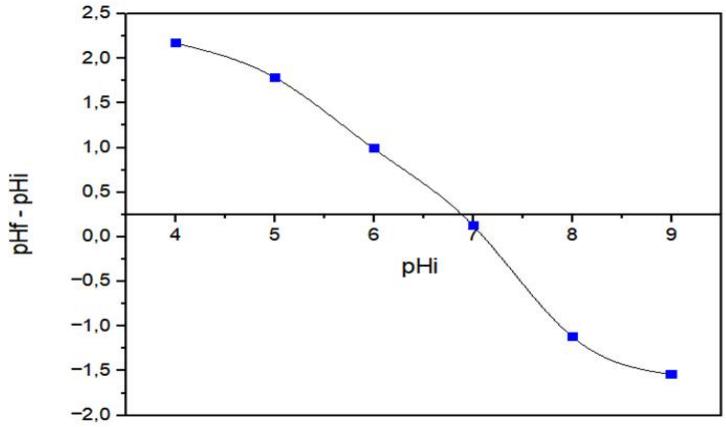

Figure III- 3: pH point of zero charge (pH_{PZC}).

The point of zero charge pH_{PZC} of the Waste foundry sand (WFS) was found to be 7.1, indicating that the adsorbent surface carries a positive charge at pH levels below 7.1 and negatively charged above this value. Since Congo Red is an anionic dye, its adsorption was more favorable in acidic conditions (pH < 7.1), where electrostatic attraction between the dye and the positively charged WFS surface is stronger. This supports the higher adsorption efficiency observed at lower pH levels during the experiments.

Both Boehm titration and pH_{PZC} measurements provided complementary results, indicating that the surface of WFS possesses mainly acidic functional groups. This explains its adsorption behavior for anionic dyes like Congo Red.

III.2. Calibration curve

The calibration curve A= f (C_0) in Figure III-4 was obtained by measuring the absorbance of the calibration solutions of Congo Red dye using UV-Vis spectrophotometer (UV iLine 9400C) at λ_{max}= 500 nm.

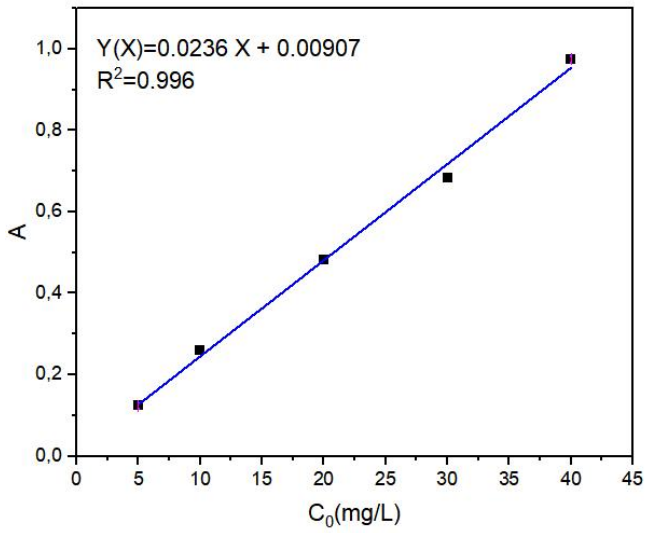

Figure III- 4: Calibration curve relative to the aqueous solution of Congo Red (CR).

The equation of curve is A= 0.0236 C_0 + 0.00907. The correlation coefficient (R^2 = 0.996) confirms excellent linearity within the tested range. This calibration curve was used to determine the residual concentrations of Congo Red in all batch adsorption experiments.

III.3. Batch Adsorption results

Table III-3 summarize the results of the Box-Behnken experimental runs, showing the effects of the selected variables on Congo Red removal efficiency

Table III- 3: Box-Behnken matrix design and the response.

Run	Factor 1 A:Concentration mg/L	Factor 2 B:WFS mass mg	Factor 3 C:pH	Response1 Q_e mg/g
1	30	20	6	5.88
2	20	20	10	3.52
3	30	30	2	13.74
4	20	30	6	6.03
5	20	30	6	5.10
6	20	20	2	26.00
7	20	40	10	10.58
8	30	40	6	3.06
9	10	40	6	2.10
10	10	30	10	0.09
11	10	20	6	1.98
12	30	30	10	1.21
13	20	30	6	9.37
14	10	30	2	6.27
15	20	40	2	12.33

III.4. Statistical modeling

III.4.1. ANOVA result

Analysis of Variance (ANOVA) is an important tool in statistical analysis. It analyses the impact of experimental parameters in affecting the response [7].

The ANOVA for the adsorption of Congo Red using WFS is presented in Table III-4 below

Table III- 4: Analysis of variance.

Source	Sum of squares	Df	Mean square	F-value	P-value	
Model	599.74	9	66.64	19.00	0.0024	Significant
A-concentration	22.61	1	22.61	6.45	0.0520	
B-WFS mass	10.83	1	10.83	3.09	0.1392	
C-pH	230.58	1	230.58	65.73	0.0005	
AB	2.15	1	2.15	0.6135	0.4689	
AC	10.08	1	10.08	2.87	0.1508	
BC	107.39	1	107.39	30.61	0.0026	
A^2	118.91	1	118.91	33.90	0.0021	
B^2	16.32	1	16.32	4.65	0.0835	
C^2	64.33	1	64.33	18.34	0.0078	
Residual	17.54	5	3.51			
Lack of fit	7.46	3	2.49	0.4933	0.7227	Not significant
Pure error	10.08	2	5.04			
Cor total	617.28	14				

We found the p-value of the model is 0.0024 which is less than 0.05 and the F-value of 19.00, those results confirms that the model is significant and it can describe the experimental data.

The lack of fit is not significant (P-value = 0.7227) indicating good agreement between experimental and predicted values.

The pH is the most affecting parameter on this adsorption with P-value of 0.0005 followed by the interaction pH* WFS mass with p-value of 0.0026 also the concentration was close to the threshold with P-value of 0.0520 suggesting some influence.

III.4.2. Regression model

It is a mathematical equation that relates the response (Q_e) to the influencing factors; it is obtained using the design expert software.

The aim of the mathematical modelisation is to be able to then calculate all the responses in the field of study without having to do the experiments.

In our case, this equation is quadratic because we have three influencing factors.

$$Q_e = +34.77883 + 2.89632 \text{ concentration} - 7.56507 \text{ pH} + 0.129537 \text{ WFS mass} * \text{pH} - 0.056750 \text{ concentration}^2 + 0.021021 \text{ WFS mass}^2.$$

The positive or negative signs of the coefficients indicate whether each variable increases or decreases the adsorption.

III.4.3. Response surface plots

To better understand the impacts and the interactions of the parameters on the adsorption of Congo Red by the WFS the 3D responses surface plots were generated using the regression model by the design expert software.

Those plots Figure III-5 show how the adsorption capacity changes with the combinations of the parameters.

(a)

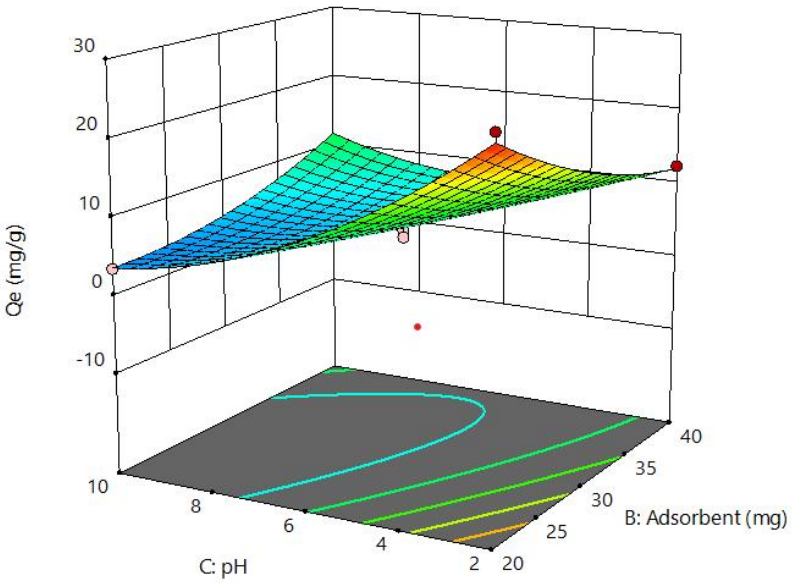

(b)

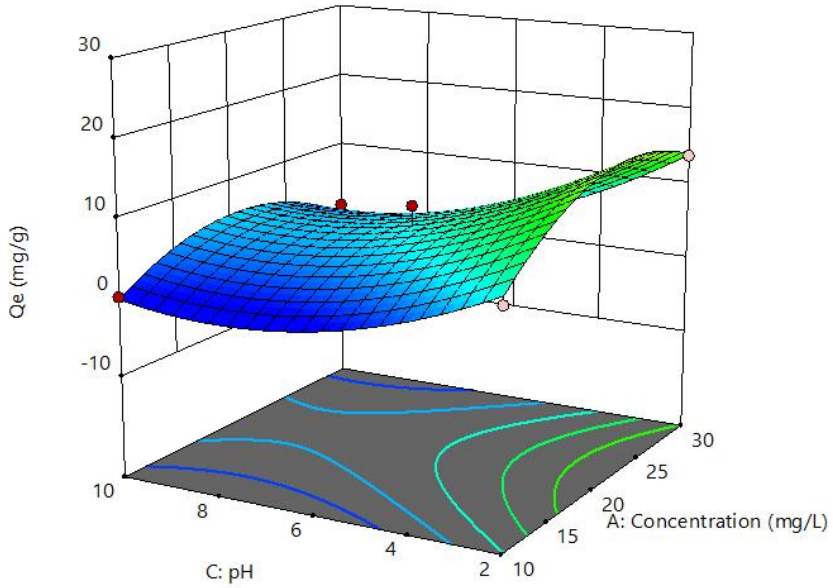

(c)

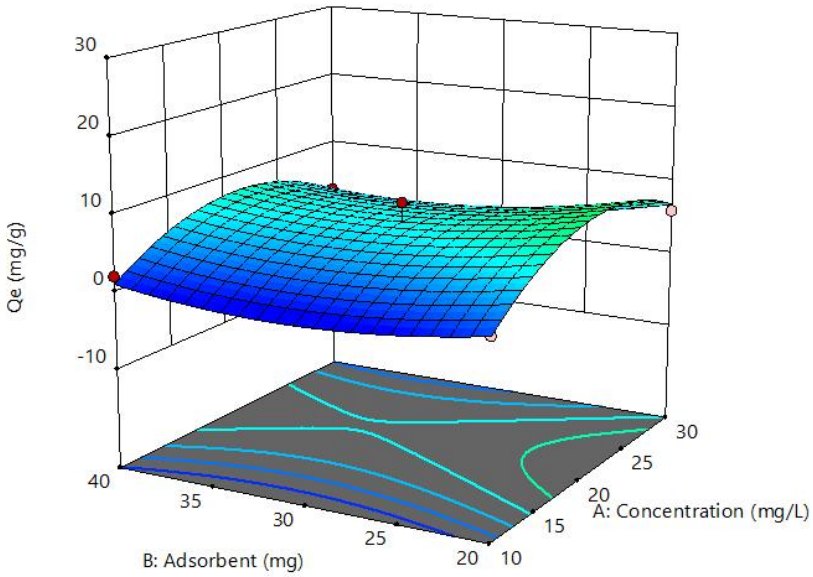

Figure III- 5: 3D response surface plots of interaction of Q_e with (a) B-mass of WFS and C-pH, (b) A-concentration and C-pH, (c) A-concentration and B-mass of WFS.

(a). We fixed the concentration ,and we changed the pH on (2,10) , mass of WFS on (20,40 mg) ,we notice that the increasment of the pH and the mass of WFS the adsorption capacity(Q_e) decrease.

The best adsorption capacity was obtained when the pH around 2 and the WFS around 20 mg.

(b). We fixed the mass of WFS and changed the pH on (2,10) and the concentration on (10,30 mg/L) , in this one we notice that the incresment of the pH decrease the Q_e ,and when we increase the concentration the Q_e increase at first then starts to drop suggesting that the optimal concentration is around 20 mg/L.

(c). We fixed the pH, and change the mass of adsorbent on (20,40 mg) and the concentration (10,30 mg/L), the same results are noted in the third graph, the better adsorption capacity is at 20 mg/L concentration and 20 mg of the WFS.

Based on the regression model and surface plots analysis, we conclude that the optimal conditions for this adsorption are:

- ✓ **pH of the solution :** 2.
- ✓ **Initial dye concentration:** 20 mg/L.
- ✓ **Mass of WFS:** 20 mg.

III.5. Kinetics study

A comparative kinetic analysis was conducted to assess the effectiveness of the two treatment approaches. The adsorption and the photocatalysis of the Congo Red by the WFS, both processes were cared under similar conditions (C_0 = 20 mg/L, pH = 2, mass of adsorbent = 20 mg).

The aim of this study was to determine which method work better and faster.

III.6. Modeling of the kinetic

In order to better understand the kinetics of the adsorption process, different mathematical models were applied to determine which one best fits this adsorption as Figure III-6 show.

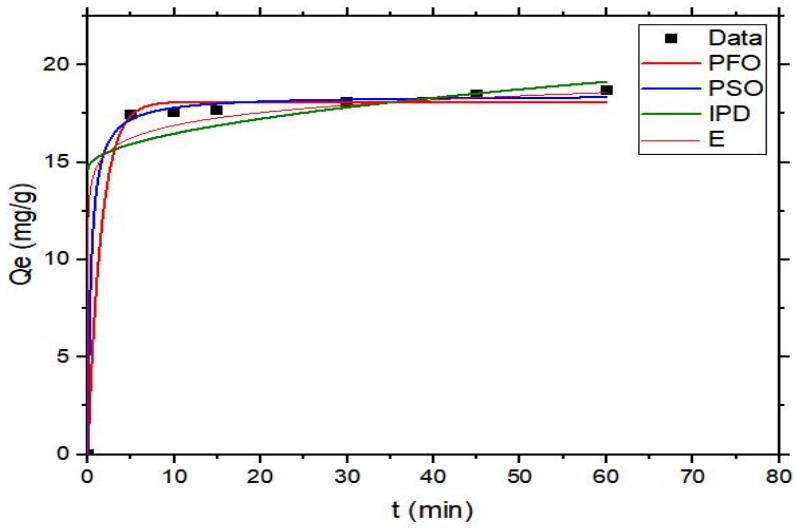

Figure III- 6: Nonlinear regression analyses for kinetic data

The adsorption kinetics parameters calculated for the adsorption of CR by WFS are presented in Table III-5.

Table III- 5: Kinetic parameters of the CR adsorption by WFS.

sample	CR
C_0 (mg/L)	20
Q_{eq}(exp) mg/g	18.70
Pseudo-first order	
K_1 (min^{-1})	0.64
Q_1 (cal)(mg/g)	18.10
R^2	0.996
RMSE%	14.86
x^2	73.21
Pseudo-second order	
K_2 (g/mg.min)	0.14
Q_2 (cal)(mg/g)	18.44
R^2	0.998
RMSE%	0.66
x^2	0.14
Elovich	
α (mg/g.min)	5878337.67
β (g/mg)	0.49
R^2	0.749
RMSE%	12.10
x^2	43.52
Intraparticle diffusion IPD	
K_{ID} (mg/g.$min^{1/2}$)	0.58
C	14.63
R^2	0.270
RMSE%	12.91
x^2	54.27

The pseudo second order model (PSO) is the best fit for the kinetic data according to the R^2 = 0.998, the small value of RMSE% = 0.66 and χ^2 = 0.14. This indicating that the interaction

between the CR molecules and the active sites of the WFS are chemical interaction (chemisorption).

These result is found with previous study [45], which also reported that the PSO model better explains the adsorption CR onto solid adsorbents.

III.7. Isotherm study

The adsorption isotherms are among the most important data to understanding the mechanism of the adsorption systems. These isotherms give in information about the adsorption capacity [12].

III.8. Modeling of adsorption isotherms

To describe the equilibrium behavior of Congo Red adsorption onto WFS, various isotherm models were applied to the experimental data. The fitting of the data to the selected isotherms is illustrated in Figure III-7, showing the relationship between the amount of dye adsorbed and its equilibrium concentration.

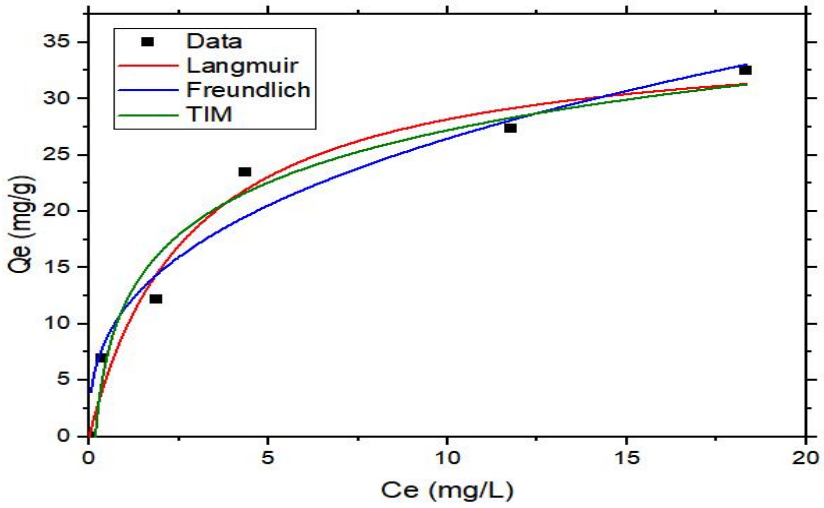

Figure III- 7: Nonlinear regression analyses for equilibrium data.

The adsorption isotherm parameters calculated for the adsorption of CR by WFS are presented in Table III-6.

Table III- 6: Isotherm parameters of the CR adsorption by WFS.

Sample	CR
Langmuir	
Q_{max} (mg/g)	36.16
K_L	0.35
R_L	0.12
R^2	0.976
RMSE%	1.93
χ^2	2.25
Freundlich	
K_F (mg/g)(mg/L)$^{1/n}$	11.37
n	2.73
R^2	0.951
RMSE%	2.08
χ^2	1.26
Temkin	
K_T (L/g)	5.82
b_T (kJ/mol)	0.36
R^2	0.972
RMSE%	2.11
χ^2	1.62

Althought the correlation coefficient of both temkin and Langmuir isotherm models were very close the error value of Langmuir were smaller (RMSE%= 1.93) indicating that the adsorption energy lowes progressively with increasing dye coverage, reflecting a Homogeneous surface and monolayer adsorption between the Congo Red molecules and the WFS surface.

These result is found with previous study [46], which also reported that the Langmuir model better explains the adsorption CR onto solid adsorbents.

III.9. Comparison of adsorption capacities of various adsorbents for removal of CR

Table III -7 presents a comparison of the adsorption capacities of various adsorbents reported in the literature for the removal of Congo Red dye, including the performance of Waste Foundry Sand (WFS) used in this study

Table III- 7: comparison of Q_e of various adsorbents.

The adsorbent	pH	Q_e(mg/g)	reference
Aspergillus niger	6	14.72	[47]
Wheatbran	8	22.73	[48]
Activatedcarbon (commercial grade)	2	0.63	[49]
Alternaria alternata	5	60.0	[50]
Pinecone	3.55	40.19	[51]
Rice husk	6	14	[52]
Orange peel	5	22.4	[53]
Illite clay	5.7	61	[54]
WFS	2	36.16	This study

The adsorbent WFS showed relatively better adsorption potential of CR dye. The availability and cost effectiveness of WFS might provide a cheap source of adsorbents for the sequestration of toxic dyes from industrial effluents.

III.10. Temperature effect

The effect of temperature on the adsorption of Congo Red onto WFS was investigated to assess the influence of thermal conditions on the adsorption process. Figure III-8 presents the variation in adsorption capacity at different temperatures.

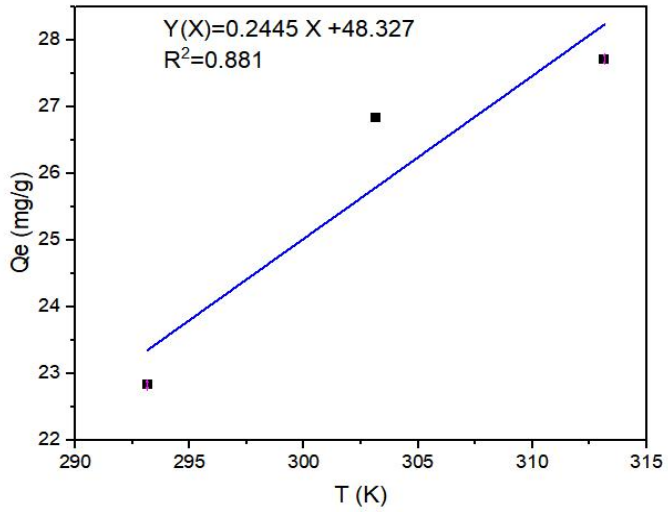

Figure III- 8: Temperature effect on the adsorption of CR by WFS

An increase in temperature corresponds with a rise in Q_e values, suggesting that the adsorption process proceeds via an endothermic mechanism, and therefore temperature control is important to improve the performance of the adsorbent.

III.11. Thermodynamic study

The thermodynamic parameters of the adsorption process were evaluated using a Van't Hoff plot. Figure III-9 present the linear relationship between ln Kc and 1/T, from which the values of the thermodynamic parameters were determined.

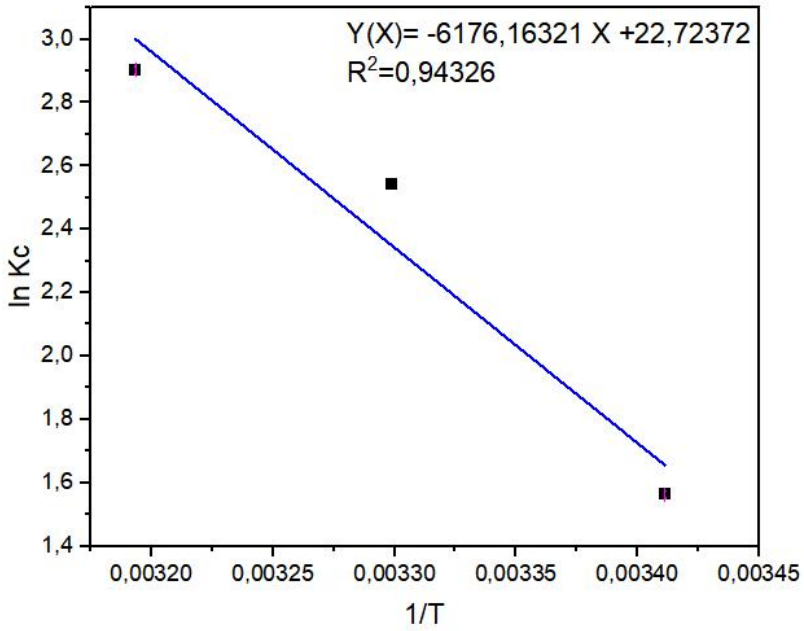

Figure III- 9: Thermodynamic study

The thermodynamic parameters were calculated and the results are presented in Table III-8 below:

Table III- 8: Thermodynamic parameters.

ΔH^0 (kJ/mol)	ΔS^0 (J/mol.K)	ΔG^0 (kJ/mol)		
		293 K	303 K	313 K
51.32	188.81	– 3.81	– 5.69	– 7.75

The ΔG° was found to be negative, indicating that the adsorption process is spontaneous. The positive value of ΔH° confirms that the process is endothermic, suggesting that higher temperatures favor the adsorption. Additionally, the positive ΔS° value implies increased disorder at the solid–liquid interface during dye adsorption.

III.12. Comparison Between Adsorption and Photocatalytic Yields

To evaluate and compare the efficiency of the two treatment methods, adsorption and photocatalysis, a comparison of their respective removal yields was carried out. Figure III-10 presents the removal efficiencies of Congo Red using both techniques under their optimized conditions.

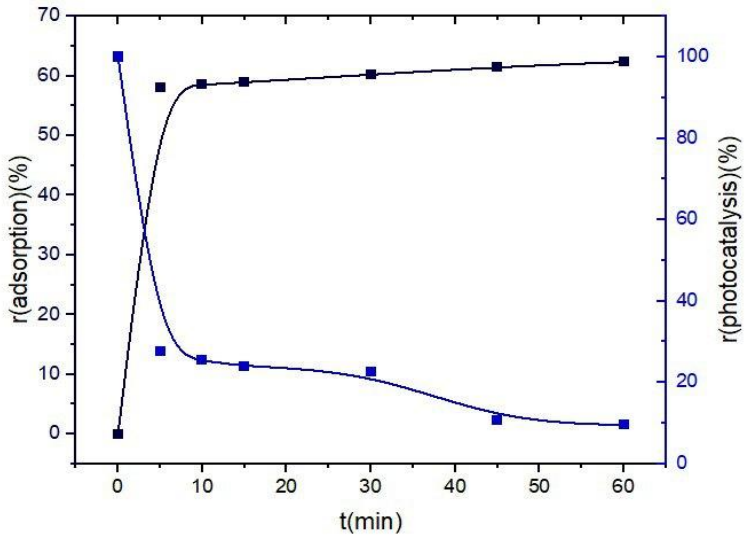

Figure III- 10: Yields comparison of the adsorption and photocatalysis processes.

The final dye removal yield at 60 min was found to be 62.34% for adsorption and 90.49% for the photocatalysis, indicating that the photocatalysis process achieved higher removal efficiency under the same experimental conditions.

General conclusion

IV. General conclusion

The aim of this study was to determine the effectiveness of waste foundry sand as a low-cost adsorbent for the removal of Congo Red dye from water using two different methods: adsorption and photocatalysis.

Experimental results revealed that photocatalysis achieved a higher CR removal efficiency with approximately 90.49%, while adsorption efficiency was 62.34%. Even though the photocatalysis was more efficient than the adsorption, the adsorption proved to be simpler and practical method under the conditions studied.

The important findings from this work:

- ✓ Characterisation analyses (XRD, FTIR, Boehm titration, and pH_{PZC}) confirmed the suitability of the WFS as a good adsorbent.
- ✓ XRD results confirmed the presence of Al_2O_3, Fe_2O_3, SiO_2, and TiO_2, indicating the crystalline structure of the WFS.
- ✓ FTIR analysis identified several notable functional groups, such as an C≡N stretch at 2355.5 cm^{-1}, a Metal carbonyl stretch at 2004.98 cm^{-1}, and a Si–O bend at 494.26 cm^{-1}.
- ✓ The pH_{PZC} value (7.1) indicated that adsorption is more favorable under acidic conditions (pH < 7.1), where the WFS surface carries a positive charge, enhancing the electrostatic interaction with the anionic dye molecules like CR .
- ✓ Boehm titration results revealed a predominance of acidic functional groups on the WFS surface, thereby enhancing its potential for strong interactions with CR.
- ✓ Kinetic analyses indicated that the adsorption process adheres to the pseudo-second-order model, implying that chemisorption governs the adsorption mechanism.
- ✓ The isotherm modeling showed that the best fit model was the Langmuir model, indicating a monolayer adsorption with a maximum capacity of 36.16 mg/g.
- ✓ The calculated thermodynamic parameters confirmed that the process was endothermic.

Finally, WFS has proved to be an effective, low-cost, and environmentally friendly adsorbent for the removal of Congo Red dye from wastewater.

References

[1] Patil, C.R.; Patil, S.A.; Tawade, A.K.; Kambale, B.B.; Tayade, S.N.; Patil, S.S.; Zambare, D.N.; 2024, Adsorptive Removal of Methylene Blue Dye by Annealed Waste Foundry Sand. *Asian Journal of Chemistry*, 36 (4), 974-982. https://doi.org/10.14233/ajchem.2024.31029

[2] Zhu,Y.; Wang, S.; Liu, Y.; Han, J. ; Duan, G.; Fu, Q.; Han, X.; Zhang, C.; He, S.; Jiang, S.;2025, Structure modifications of wood-based materials for water treatment applications: A review. *Materials Today*, 87, 252-286. https://doi.org/10.1016/j.mattod.2025.04.012

[3] Sajai, N.; Soubai, B.; El Khaider, S.; Chham, A.; Fakhreddine, R.; Mechnou, I.; Krimi, S.; 2025, Valorization of calcium phosphate glasses: A sustainable and eco-friendly approach to methylene blue dye adsorption from wastewater. *Results in Surfaces and Interfaces*, 19, 100525. https://doi.org/10.1016/j.rsurfi.2025.100525

[4] Batana, F.Z.; Bouras, H.D.; Aouissi, H.; 2022, Biosorption of Congo red and Basic fuchsin using micro-fungi Fusarium oxysporum f. sp. pisi as a biosorbent: Modeling, optimization and kinetics study. *Egyptian Journal of Chemistry*, 65, 225–235. 10.21608/ejchem.2022.113994.5188

[5] Nagraj; Chaurasia, P.K.; Bharati, S.L.; Sharma, N.; Kumar, J.; Sivalingam, A.M.; 2025, Degradation of dyes by fungi: An overview on recent updates. *The Microbe*, 6, 100232. https://doi.org/10.1016/j.microb.2024.100232

[6] Bouras, H.D.; Yeddou, A.R.; Bouras, N.; Chergui, A.; Favier, L.; Amrane, A., and Dizge, N.;2021, Biosorption of cationic and anionic dyes using the biomass of *Aspergillus parasiticus* CBS100926^{T}. *Water Science & Technology*, 83 (3), 622-630. https://doi.org/10.2166/wst.2021.005

[7] Ng, Y.S.; Gupta, B.S.; Hashim, M.A.; 2014, Performance evaluation of natural iron-rich sandy soil as a low-cost adsorbent for removal of lead from water. *Desalination and Water Treatment*, 57, 5013–5024. https://doi.org/10.1080/19443994.2014.999711.

[8] Eskikaya, O.; Arslan, H.; Gün, M.; Bouras, H.D.; Dizge, N.; 2022, Preparation of bio-based adsorbent from waste tomato stem and used as photocatalyst for Basic Red 2 photocatalysis. *Research Square (preprint)*, DOI:10.21203/rs.3.rs-1647278/v1

[9] García, G.; Cabrera, R.; Rolón, J.; Pichardo, R.; and Thomas, C.; 2024, Systematic review on the use of waste foundry sand as a partial replacement of natural sand in concrete.

Construction and Building Materials, 430, 136460. https://doi.org/10.1016/j.conbuildmat.2024.136460.

[10] Tittarelli, F.; 2018, Waste foundry sand. *Waste and Supplementary Cementitious Materials in Concrete*, 121–147. https://doi.org/10.1016/B978-0-08-102156-9.00004-3

[11] Siddique, R.; Singh, G.; 2011, Utilization of waste foundry sand (WFS) in concrete manufacturing, Resources. *Conservation and Recycling*, 55, 885–892. https://doi.org/10.1016/j.resconrec.2011.05.001

[12] Gürkan, E.H.; Çoruh, S.; 2018, Using waste foundry sand for the removal of malachite green dye from aqueous solutions - Kinetic and equilibrium studies. *Environmental Engineering and Management Journal*, 17 (1), 123–133. DOI:10.30638/eemj.2018.014

[13] Benkhaya, S.; M'rabet, S.; and El Harfi, A.; 2020, A review on classifications, recent synthesis and applications of textile dyes. *Inorganic Chemistry Communications*, 115, 107891. https://doi.org/10.1016/j.inoche.2020.107891

[14] Amourache-Benazzouz, M.; 2019, Étude de l'élimination du bleu de méthylène et de composés organiques toxiques à partir de solutions aqueuses par un biosorbant non conventionnel, Claviceps purpurea hébergé par Elytrigia repens L: Implications sur la dépollution de l'eau et cas d'études, Doctoral thesis, Dept. Sciences de la Matière, Université 8 Mai 1945 Guelma, Guelma, Algeria.

[15] Berradi, M.; Hsissou, R.; Khudhair, M.; Assouag, M.; Cherkaoui, O.; El Bachiri, A.; El Harfi, A.; 2019, Textile finishing dyes and their impact on aquatic environs. *Heliyon*, 5, e02711. https://doi.org/10.1016/j.heliyon.2019.e02711

[16] Sharma, J.; Sharma, S.; Soni, V.; 2021, Classification and impact of synthetic textile dyes on Aquatic Flora: A review. *Regional Studies in Marine Science*, 45, 101802. https://doi.org/10.1016/j.rsma.2021.101802

[17] Affat, S.S.; 2022, Classifications, Advantages, Disadvantages, Toxicity Effects of Natural and Synthetic Dyes: A review. *University of Thi-Qar Journal of Science* (UTsci), 8 (1), 130–135.

[18] JessieRaj, M.B.; and Pavithra, M.; 2024, Prompt photocatalytic purification of dye wastewater using zinc doped nickel oxide nanostructures and Artemia salina model for acute

toxicity screening. *Next Nanotechnology*, 7, 100117, https://doi.org/10.1016/j.nxnano.2024.100117

[19] Bechki, M.K.; 2018, Préparation et caractérisation du charbon actif à partir des noyaux du palmier dattier et des coquilles des noix, Doctoral thesis, Dept. Chimie, Univ. Kasdi Merbah Ouargla, Ouargla, Algeria.

[20] García-Rollán, M.; Sanz-Santos, E.; Belver, C.; Bedia, J.; 2025, Key adsorbents and influencing factors in the adsorption of micro- and nanoplastics: A review. *Journal of Environmental Management*, 383, 125394. https://doi.org/10.1016/j.jenvman.2025.125394

[21] Chouchane, T.; 2009, Synthèse, caractérisation et application de matériaux catalytiques, Doctoral thesis, Dept. of Chemistry, Université Badji Mokhtar – Annaba, Algeria.

[22] Berez, A.; 2015, Dépollution par l'argile naturelle d'effluents teinturiers: étude expérimentale et modélisation du processus d'adsorption/désorption en réacteur fermé et colonne de percolation, Doctoral thesis, Université de Strasbourg and Université de Carthage, France and Tunisia.

[23] Bouaziz, M.G.; 2023, Étude de la rétention du cuivre en solutions aqueuses par une bentonite de Mostaganem modifiée, Doctoral thesis, Dept. of Civil and Hydraulic Engineering, Université Mohamed Khider – Biskra, Algeria.

[24] Bencheqroun, Z.; 2021, Étude de l'adsorption des colorants textiles simples ou mélangés sur des matériaux naturels: mode batch et dynamique, Doctoral thesis, Centre d'Études Doctorales – Sciences et Techniques de l'Ingénieur, Faculté des Sciences et Techniques de Fès, Université Sidi Mohamed Ben Abdellah, Morocco.

[25] Benkartoussa, M.; 2021, Utilisation de bio-sorbants dans l'adsorption de plus d'un polluant, Doctoral thesis, Dept. of Environmental Engineering, Université de Constantine 3, Algeria.

[26] Haou, S.; 2023, Etude et Modélisation de la sorption des colorants contenu dans les effluents industriels, Doctoral thesis, Université Badji Mokhtar - Annaba, Dept. de Génie des Procédés, Annaba, Algeria.

[27] Musah, M.; Azeh, Y.; Mathew, J.T.; Umar, M.T.; Abdulhamid, Z.; and Muhammad, A. I.; 2022, Adsorption kinetics and isotherm models: A review. *Caliphate Journal of Science & Technology (CaJoST)*, 1, 20–26, https://doi.org/10.4314/cajost.v4i1.3

[28] Benjelloun, M.; Miyah, Y.; Evrendilek, G.A.; Zerrouq, F.; and Lairini, S.; 2021, Recent advances in adsorption kinetic models: Their application to dye types. *Arabian Journal of Chemistry*, 14, 103031, https://doi.org/10.1016/j.arabjc.2021.103031

[29] Vareda, J.P.; 2023, On validity, physical meaning,mechanism insights and regression of adsorption kinetic models. *Journal of Molecular Liquids*, 376, 121416 , https://doi.org/10.1016/j.molliq.2023.121416

[30] Mandade, P.; 2021, Introduction, basic principles, mechanism, and challenges of photocatalysis, in Handbook of Nanomaterials for Wastewater Treatment, 1st ed., Amsterdam, Netherlands: Elsevier, 5, 137–153. https://doi.org/10.1016/B978-0-12-821496-1.00016-7

[31] Náfrádi, M.; Veréb, G.; Firak, D.S.; and Alapi, T.; 2022, Photocatalysis: Introduction , mechanism, and effective parameters, *Green Photocatalytic Semiconductors*, Garg, S.; and Chandra, A.; Green Chemistry and Sustainable Technology, Cham, Switzerland: Springer Nature Switzerland AG, (1), 3–26. DOI:10.1007/978-3-030-77371-7_1

[32] Choi, J.; 2009, Introduction and summary, in Visible-Light Active Photocatalysts for Environmental Applications and Hydrogen Production, Doctoral Thesis, California Institute of Technology, Pasadena, CA, USA.

[33] Bopape, D.A.; Ntsendwana, B.; and Mabasa, F.D.; 2024, Photocatalysis as a pre-discharge treatment to improve the effect of textile dyes on human health: A critical review. *Heliyon*, 10, 2405-8440. https://doi.org/10.1016/j.heliyon.2024.e39316

[34] Arun, J.; Nachiappan, S.; Rangarajan, G.; Alagappan, R. P.; Gopinath, K.P.; Lichtfouse, E.; 2023, Synthesis and application of titanium dioxide photocatalysis for energy, decontamination and viral disinfection: a review. *Environmental Chemistry Letters*, 21, 339–362. DOI: 10.1007/s10311-022-01503-z

[35] Villa, K.; Galán-Mascarós, J.R.; López, N.; Palomares, E.; 2021, Photocatalytic water splitting: advantages and challenges. *Sustainable Energy & Fuels*, 5 (17), 4380–4402. https://doi.org/10.1039/D1SE00808K

[36] Bakhtiar, A.; 2022, Élaboration de photocatalyseurs à base d'argile pour la décontamination des polluants organiques en solution aqueuse, Doctoral Thesis, Univ. de Lille and Univ. des Sciences et de la Technologie d'Oran Mohamed-Boudiaf (USTO-MB), France and Algeria.

[37] Zeghioud, H.; 2018, Dégradation photocatalytique de colorants présents dans les effluents textiles - Intérêt du couplage photocatalyse/biodégradation, Doctoral Thesis, Dept. Génie des Procédés, Université Badji Mokhtar-Annaba, Annaba, Algeria.

[38] Mebrek, A.; 2018, Élaboration et caractérisation de céramiques ZnO–TiO_2, Doctoral thesis, Dept. of Physics, Université Badji Mokhtar–Annaba, Annaba, Algeria.

[39] Yon, V.; 2021, Advanced X-ray characterization for the development of low consumption power transistors, Doctoral thesis, Université Grenoble Alpes – CEA-Leti, France.

[40] Mohammed, A.; Abdullah, A.; 2018, Scanning electron microscopy (SEM): A review. *Proceedings of 2018 International Conference on Hydraulics and Pneumatics - HERVEX*, 130, 77–85.

[41] Jegan, J.; Praveen, S.; Kumar, B.M.; Pushpa, T.B.; Gokulan, R.; 2021, Box– Behnken experimental design for the optimization of Basic Violet 03 dye removal by groundnut shell derived biochar. *Desalination and Water Treatment*, 209, 379–391. https://doi.org/10.5004/dwt.2021.26495

[42] Ogunleye, O.O.; Eletta, O.; and Akinyemi, AF.; 2017, Adsorption of Congo red dye onto coconut shell based NaOH activated carbon: Kinetics, thermodynamics and optimisation studies. *Journal of engineering and technology*, 3 (1), 105 - 116.

[43] Cammelli, F.; Tameni, G.; Bernardo, E.; 2024, Sustainable stabilization of waste foundry sands in alkali activated glass-based matrices. *Case Studies in Construction Materials*, 21 (2), e03538. https://doi.org/10.1016/j.cscm.2024.e03538

[44] Zhang, M.; Liu, X.; Li, W.; Tan, Z.; Wang, Q.; Zhang, L.; 2021, Removal of toxic dyes from aqueous solutions by adsorption onto a novel activated carbon prepared from chestnut shell. *Desalination and Water Treatment*, 222, 246–258. https://doi.org/10.5004/dwt.2021.27083.

[45] Garud, H.B.; Patil, P.H.; Jadhav, S.A.; Patil, P.S.; Kalantre, V. A.; Burungale, S.H.; 2025, Effective removal of dyes from their mixture in solution by waste-derived microadsorbents: Physicochemical characterization and adsorption removal studies. *Next Research*, 2 (2), 100235. https://doi.org/10.1016/j.nexres.2025.100235

[46] Bouras, H.D.; Yeddou, A.R.; Bouras, N.; Hellel, D.; Holtz, M.D.; Sabaou, N.; Chergui,

A.; Nadjemi, B.; 2017, Biosorption of Congo red dye by Aspergillus carbonarius M333 and Penicillium glabrum Pg1: Kinetics, equilibrium and thermodynamic studies. *Journal of the Taiwan Institute of Chemical Engineers*, 80, 915–923. https://doi.org/10.1016/j.jtice.2017.08.002

[47] Ilyas, S.; Rehman, A.; 2013, Decolorization and detoxification of Synozol red HF-6BN azo dye, by *Aspergillus niger* and *Nigrosporasp*. *Iranian Journal of Environmental Health Science & Engineering*, 10 (1), 12. https://doi.org/10.1186/1735-2746-10-12

[48] Wang, X.S.; Chen, J.P.; 2009, Biosorption of Congo Red from Aqueous Solution using Wheat Bran and Rice Bran: Batch Studies. *Separation Science and Technology*, 44 (6), 1452–1466. https://doi.org/10.1080/01496390902766132

[49] Khambhaty, Y.; Mody, K.; Basha, S.; 2012, Efficient removal of Brilliant Blue G (BBG) from aqueous solutions by marine Aspergillus wenttii: Kinetics, equilibrium and process design. *Ecological Engineering*, 41, 74–83. https://doi.org/10.1016/j.ecoleng.2012.01.002

[50] Chakraborty, S.; Basak, B.; Dutta, S.; Bhunia, B.; Dey, A.; 2013, Decolorization and biodegradation of congo red dye by a novel white rot fungus Alternaria alternata CMERI F6. *Bioresource Technology*, 147, 662–666. https://doi.org/10.1016/j.biortech.2013.08.117

[51] Dawood, S.; Sen, T.K.; 2012, Removal of anionic dye Congo red from aqueous solution by raw pine and acid-treated pine cone powder as adsorbent: Equilibrium, thermodynamic, kinetics, mechanism and process design. *Water Research*, 46 (6), 1933–1946. https://doi.org/10.1016/j.watres.2012.01.009

[52] Han, R.; Ding, D.; Xu, Y.; Zou, W.; Wang, Y.; Li, Y.; Zou, L.; 2008, Use of rice husk for the adsorption of congo red from aqueous solution in column mode, *Bioresource Technology*, 99 (8), 2938-2946. https://doi.org/10.1016/j.biortech.2007.06.027

[53] Namasivayam, C.; Muniasamy, N.; Gayatri, K.; Rani, M.; Ranganathan, K.; 1996, Removal of dyes from aqueous solutions by cellulosic waste orange peel. *Bioresource Technology*, 57 (1), 37-43. https://doi.org/10.1016/0960-8524(96)00044-2

[54] Altaie, O.T.S.; Zeidan, H.; Karakaya, N.; Karakaya, M.Ç.; Marti, M.E.; 2023, Removal of Congo red from aqueous solutions by adsorption onto illite clay. *Desalination and Water Treatment*, 310, 226-237. https://doi.org/10.5004/dwt.2023.29941

Annex

الجمهورية الجزائرية الديمقراطية الشعبية
People's Democratic Republic of Algeria
وزارة التعليم العالي والبحث العلمي
Ministry of Height Education and Scientific research

University of Ghardaia
Faculty of Sciences and Technology
Department of Common Teaching in Sciences and Technology

جامعة غرداية
كلية العلوم والتكنولوجيا
قسم التعليم المشترك في العلوم والتكنولوجيا

Approval for Final Printing of a Master's Dissertation

	Name and Surname	Signature
Examiner 1	Mounir DAOUD	
Examiner 2	Yasmina KHANE	
Supervisor	Hadj Daoud BOURAS	
Co-Supervisor	//////////////////////////////////	//////////////////////////////////

I, the undersigned, Mrs: .Zohra BABAAMER

President of the jury for the student(s): Romaissa DAHEUR and Ibtissem HABIB

Field: Chemistry; **Specialization:** Analytical Chemistry

Thesis Title: Experimental study on the removal of Congo Red by adsorption using waste foundry sand.

Hereby authorize the above-mentioned student(s) to print and submit their final manuscript to the department.

Ghardaia: 18/06/2025

President of the jury

Head of the department

رئيس قسم التعليم المشترك
في العلوم والتكنولوجيا
شعوبية فيصل

جامعة غرداية
قسم التعليم المشترك في العلوم والتكنولوجيا
كلية العلوم و التكنولوجيا